Acta Geochim (2018) 37(6):820–841
https://doi.org/10.1007/s11631-018-0288-1

ORIGINAL ARTICLE

Origin and genetic family of Huhehu oil in the Hailar Basin, northeast China

Yao-Ping Wang[1,2] · Fan Zhang[3] · Yan-Rong Zou[1] · Zhao-Wen Zhan[1] · Yulan Cai[1]

Received: 25 January 2018 / Revised: 20 May 2018 / Accepted: 6 July 2018 / Published online: 17 July 2018

Abstract The Huhehu Sag is one of the most important oil and gas depressions in the Hailar Basin. However, the origin of Huhehu oil is still controversial. Previous studies on source rocks have mainly focused on the Nantun Formation (K_1n); a few studies have investigated the Damoguaihe Formation (K_1d). Based on the Rock–Eval pyrolysis parameters, 172 drill cutting samples from the Huhehu Sag were analyzed to evaluate their geochemical characteristics. Based on the Rock–Eval data, the mudstones from the first member of the Damoguaihe Formation (K_1d_1) and the second member of the Nantun Formation (K_1n_2) have moderate to high hydrocarbon generation potential, while mudstones from the first member of the Nantun Formation (K_1n_1) have poor to good hydrocarbon generation potential. Additionally, both the K_1n_1 and K_1n_2 coal members have poor to fair hydrocarbon generation potential, but the K_1n_2 coal member has a better generative potential. Fifteen Huhehu oils were collected for molecular geochemical analyses to classify the oils into genetic families and to identify the source rock for each oil using chemometric methods. The Huhehu oils were classified into three groups with different maturity levels using hierarchical cluster analysis and principal component analysis. Group A oils (high maturity) are characterized by relatively moderate ratios of Pr/Ph, Pr/n-C_{17}, and Ph/n-C_{18}, as well as an abundance of C_{29} steranes, mainly derived from the K_1n_2 and K_1n_1 mudstone members. In comparison, group B oils (moderate maturity) have relatively low Pr/Ph ratios, moderate Pr/n-C_{17} and Ph/n-C_{18} ratios, and low concentrations of C_{29} steranes. Group C oils (low maturity) show relatively high ratios of Pr/Ph, Pr/n-C_{17}, and Ph/n-C_{18}, as well as high concentrations of C_{29} steranes. Furthermore, group B oils derived from the K_1d_1 mudstone member and group C oils derived from the K_1n_2 coal member were also identified by principal component analysis score plots. Correlation studies suggest a major contribution from the K_1n mudstone Formation and the K_1d_1 mudstone member to the oils of the Huhehu Sag. So, the Nantun Formation and relatively shallow strata of the Damoguaihe Formation (e.g., the K_1d_1 member) represent important targets for future oil-reservoir exploration in the Huhehu Sag.

Keywords Hailar Basin · Huhehu Sag · Biomarkers · Chemometrics · Oil–oil and oil–source rock correlations

1 Introduction

The Hailar Basin is the second largest continental petroliferous basin in the Daqing oil area in China and forms within a Paleozoic fold basement (Wang et al. 2009; Fig. 1a). By the end of 2014, the Huhehu Sag, located in the southeastern part of the Hailar Basin (Fig. 1b), had three low-yield oil wells (Chen 2014). In addition, the Huhehu Sag has received a great deal of attention due to its high quality of source rocks and the large potential of coalbed gases (Cui et al. 2007; Yang et al. 2008; Zhang 2014).

✉ Yan-Rong Zou
zouyr@gig.ac.cn

1 State Key Laboratory of Organic Geochemistry, Guangzhou Institute of Geochemistry, Chinese Academy of Sciences, Guangzhou 510640, People's Republic of China

2 University of Chinese Academy of Sciences, Beijing 100049, People's Republic of China

3 Exploration and Development Research Institute of Daqing Oilfield, PetroChina, Daqing 163712, People's Republic of China

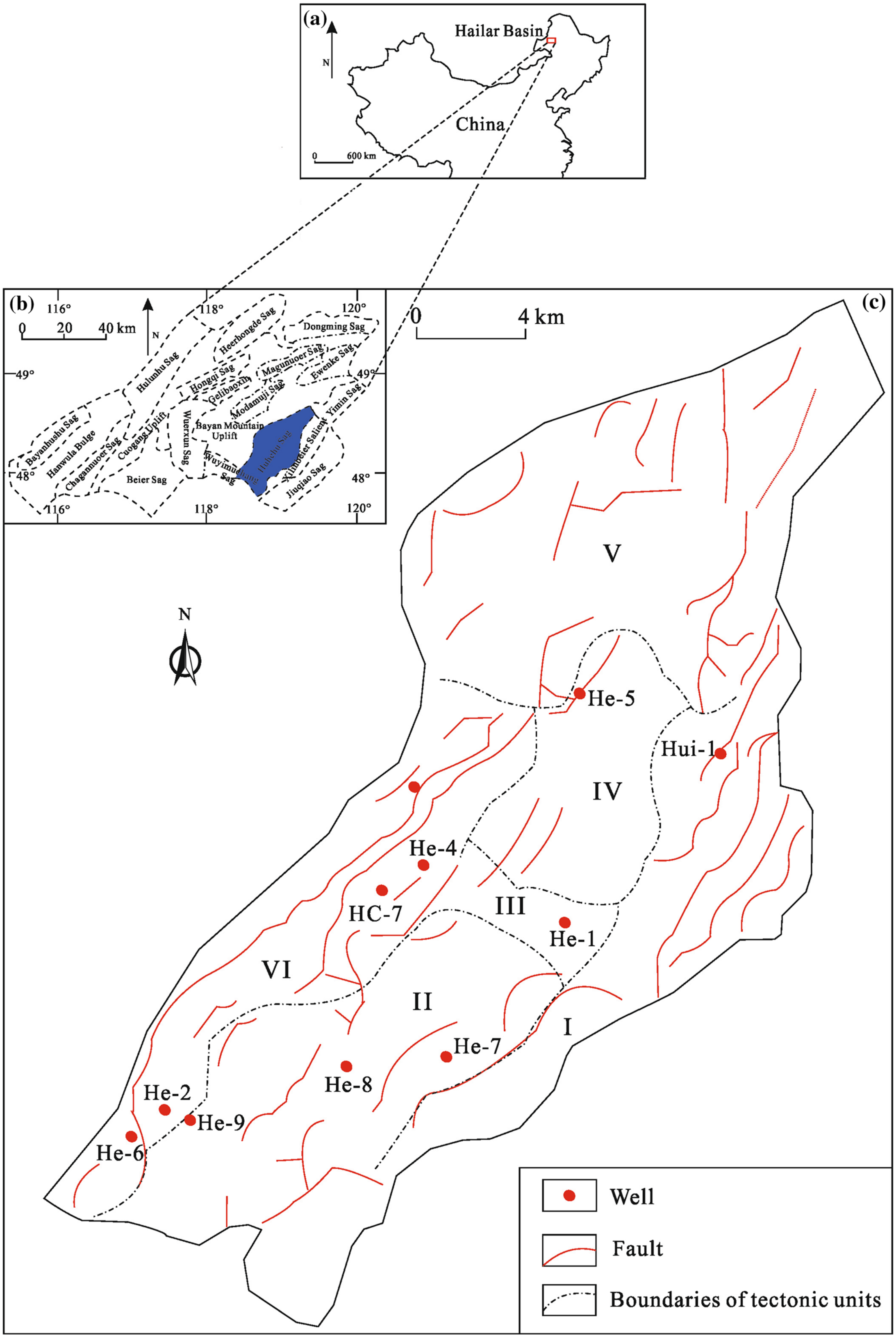

Fig. 1 Maps of **a** the Hailar Basin, and **b** Huhehu Sag, and **c** well distribution in the study area (Chen et al. 2011). I: southeast steep slope zone, II: south depression zone, III: central salient zone, IV: north depression zone, V: north slope zone, and VI: northwest gentle slope zone

Previous studies have confirmed that the study area has three sets of source rocks: the K_1d_1 member (the first member of the Damoguaihe Formation), the K_1n_2 member (the second member of the Nantun Formation), and the K_1n_1 member (the first member of the Nantun Formation) (Li et al. 2009; Lu et al. 2010; Wu and Li 2012). These source rocks are all Cretaceous (Fig. 2). Only limited oil–source rock correlation studies have been conducted in the Huhehu Sag, and the origin of Huhehu oil remains controversial (Lu et al. 2010; Chen 2014). Lu et al. (2010) found that the Huhehu oils have a good correlation with the K_1n_2 member (both mudstone and coal), while H Chen (2014) suggested that the Huhehu oils are mainly derived from the K_1n_2 coal member and the K_1n_1 mudstone member. Many publications have documented the Nantun Formation in detail in terms of molecular characteristics (Cao et al. 2010; Lu et al. 2010), organic matter enrichment, and kerogen type (Dong et al. 2011; Wu and Li 2012), but little is known about the quality of the Damoguaihe Formation. Accordingly, the present study aimed to comprehensively evaluate the source rocks of the Huhehu Sag (including the K_1d_1, K_1n_2, and K_1n_1 members) in terms of organic matter enrichment, kerogen type, depositional environment, and thermal maturity. In addition, chemometric methods were applied to determine detailed oil–oil and oil–source rock correlations. The methods used [mainly hierarchical cluster analysis (HCA) and principal component analysis (PCA)] have been widely employed in the field of environmental science for analyzing water chemistry data (Amiri et al. 2017; Ding et al. 2017) and have proven reliable in analyzing oil–oil and oil–source rock correlations (Telnæs and Cooper 1991; Chakhmakhchev et al. 1996; Zumberge et al. 2005; Peters et al. 2007, 2008, 2013, 2016; Hao et al. 2009, 2010, 2011; He et al. 2012; Wang et al. 2016, 2018; Brito et al. 2017).

2 Geological setting

The Huhehu Sag, a secondary tectonic unit of the Hailar Basin (Cao et al. 2010; Chen et al. 2011), extends northeast and has a large potential for hydrocarbon exploration (Wu and Li 2012). The Huhehu Sag is bounded by the Xilinbeier Salient, Bayan Mountain Uplift, Yimin Sag, and Tamtsag Basin of Mongolia, which lie to the east, west, south, and north, respectively (Li et al. 2010). The Huhehu Sag can be further divided into: the southeast steep slope zone (I), south depression zone (II), central salient zone (III), north depression zone (IV), north slope zone (V), and northwest gentle slope zone (VI) (Chen et al. 2011; Fig. 1c).

The Huhehu Sag covers an area of 2500 km^2 at a maximum burial depth as high as 4600 m (Li et al. 2010). The Huhehu Sag has undergone three stages in tectonic evolution (Fig. 2): the extensional faulted-depression stage, the thermal subsidence fault-depression stage, and the late depression stage (Chen et al. 2007). The Huhehu Sag is mainly filled with a Cretaceous sediment sequence, which from bottom to top is as follows: the Tongbomiao Formation (K_1t), Nantun Formation (K_1n), Damoguaihe Formation (K_1d), Yimin Formation (K_1y), and Qingyuangang Formation (K_2q). A detailed lithology of these different formations is shown in Fig. 2. The Qingyuangang Formation is composed of mudstone interbedded with sandy conglomerate. This sequence unconformably overlies the Yimin Formation. The Yimin Formation is characterized by sandstone and coal interbedded with mudstone in the lower part, and sandy conglomerate interbedded with sandstone and mudstone in the upper part (including the K_1y_3 and K_1y_2 members). The Yimin Formation conformably overlies the Damoguaihe Formation. The Damoguaihe Formation is composed of coal, sandstone, and sandy conglomerate in the upper part, and dominated by mudstone in the lower part. The Damoguaihe Formation displays an unconformable contact with the underlying Nantun Formation. An argillite-dominated lithology comprising mudstone, sandstone, coal, and sandy conglomerate constitutes the Nantun Formation. The Nantun Formation conformably overlies the Tongbomiao Formation. The Tongbomiao Formation consists of sandstone, sandy conglomerate, and mudstone.

3 Samples and methods

3.1 Samples

We collected 155 mudstone and 17 coal samples for Rock–Eval pyrolysis. The samples were from the K_1d_1 (45 samples), K_1n_2 (62 samples), and K_1n_1 (65 samples) members exposed in nine wells distributed throughout the sag. Additionally, 15 oil samples, collected from the He-2, He-6, and He-9 wells, were analyzed using gas chromatography–mass spectrometry (GC–MS) to assess their molecular characteristics.

3.2 Rock–Eval pyrolysis and bitumen extraction of source rocks

Before the Rock–Eval analysis and bitumen extraction, all drill cutting samples were cleaned using redistilled water. The samples were subsequently dried at 60 °C and crushed into powder. The powder samples were analyzed (using IFP Rock–Eval 6) for total organic carbon (TOC), hydrogen index (HI), and hydrocarbon generation potential ($S_1 + S_2$). The powder samples were initially heated to

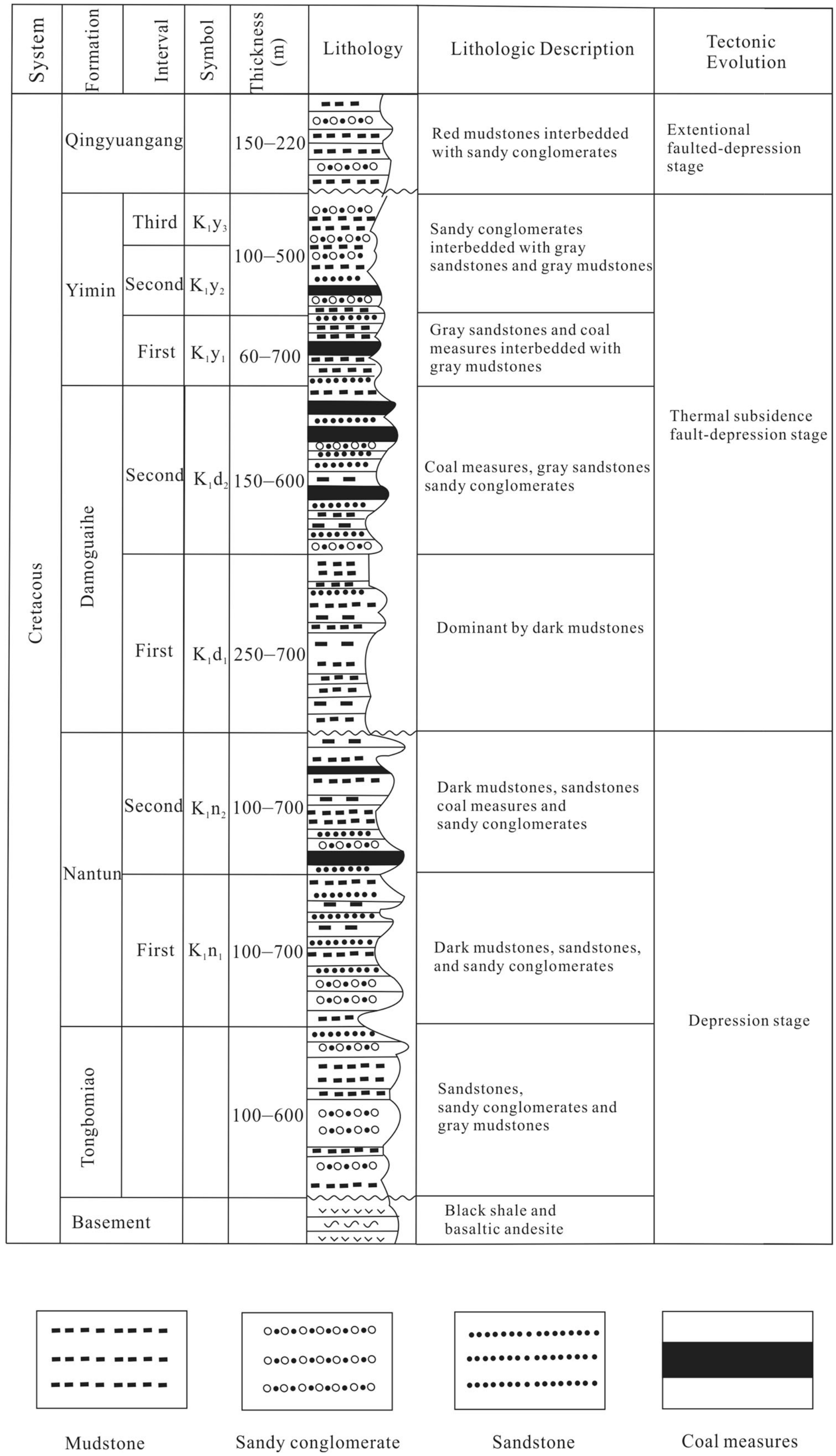

Fig. 2 Generalized stratigraphic column for the Huhehu Sag (Wu and Li 2012)

300 °C for 3 min to yield the Rock–Eval S_1 peak that represents the amount of free hydrocarbons, and then heated to 650 °C at a rate of increase of 25 °C/min to produce the Rock–Eval S_2 peak that represents the hydrocarbons generated from kerogen cracking. The temperature (°C) at which the maximum hydrocarbon yield generated from kerogen cracking occurred is T_{max}. Following pyrolysis, the pyrolyzed samples were heated from 300 to 850 °C at a rate of 20 °C/min in an oxidation furnace of the Rock–Eval 6 instrument to obtain the residual organic and inorganic carbon content. Bitumen was extracted from source rocks using a Soxhlet apparatus for 72 h with dichloromethane (DCM) mixed with methanol (93:7). All extracts and oils were separated into saturated, aromatic, and resin fractions using column chromatography.

3.3 Gas chromatography–mass spectrometry

GC–MS analyses were performed for the saturated fraction in the oils and source-rock extracts using a Thermo Fisher Trace GC Ultra gas chromatography coupled to a DSQ II mass spectrometer, equipped with a capillary column (60 m × 0.25 mm × 0.25 μm). The carrier gas was helium. The GC oven was initially kept at 60 °C for 1 min, then increased to 220 °C at a rate of 8 °C/min, then to 300 °C at a rate of 2 °C/min, and finally held at 300 °C for 25 min.

The mass spectrometer was operated at an ion source temperature of 230 °C and ionization energy of 70 eV. The analysis was conducted using mode-combining selective ion monitoring (SIM) with full-scan detection with a scan range of 50–550 Da.

3.4 Chemometric analysis

In this study, chemometric methods including HCA and PCA were applied to oil–oil and oil–source rock correlations in the Huhehu Sag. HCA and PCA are two common techniques used for chemometric exploratory data (Peters et al. 2005). Additionally, biomarker parameters, such as tricyclic terpanes, pentacyclic terpanes, and regular steranes (Peters et al. 2007, 2013), are commonly used in HCA and PCA. This study used nine source-related biomarker parameters for HCA and PCA, mainly including pentacyclic terpanes and regular steranes such as Pr/Ph, Ts/(Ts + Tm), H29/H30, C_{35}/C_{34}, Ga/C_{31}R, S/H, %C_{27}, %C_{28}, and %C_{29}, owing to the low abundance of tricyclic terpanes. These selected parameters are less likely to be affected by biodegradation, thermal maturity, and migration (Seifert and Moldowan 1978), similar to previous studies (Peters et al. 2007, 2013; Wang et al. 2016, 2018). Both HCA and PCA were completed using a commercial chemometrics program (Pirouette 4.5, Infometrix Inc., Woodinville, WA, USA). HCA was performed by range scale preprocessing, Euclidean metric distance, and incremental linkage. The PCA simplified multiple variables into a few new independent variables. Before PCA, the data were also range scaled as for HCA. The selected biomarker parameters for PCA were the same as those for HCA.

4 Results and discussion

4.1 Hydrocarbon potential and kerogen type of source rocks

The TOC contents of the mudstone samples for the K_1d_1, K_1n_1, and K_1n_2 members ranged from 1.46 to 4.27 wt% (45 samples, mean = 2.22 wt% and standard deviation = 0.66), 0.16 to 9.80 wt% (61 samples, mean = 1.71 wt% and standard deviation = 1.79), and 0.65 to 9.08 wt% (49 samples, mean = 2.82 wt% and standard deviation = 1.74), respectively (Tables 1, 2, 3). The TOC contents of the K_1n_1 and K_1n_2 coal members are in the range of 12.11–40.57 wt% (4 samples, mean = 28.72 wt% and standard deviation = 11.70) and 23.00–73.30 wt% (13 samples, mean = 49.99 wt% and standard deviation = 16.37), respectively (Tables 1, 2 and 3). The TOC contents of most K_1d_1 and K_1n_2 mudstone samples are > 2 wt%, while those of the K_1n_1 mudstone samples are generally between 1 and 2 wt%. The genetic potential ($S_1 + S_2$) is mostly between 2 and 6 mg HC/g rock for the K_1d_1 and K_1n_2 mudstone members, but is generally < 2 mg HC/g rock for the K_1n_1 mudstone member. It is noteworthy that the Huhehu Sag is a coal-rich basin, and the source rocks of the K_1d and K_1n Formations belong to typical coal-bearing strata (Chen 2014; Zhang 2014). Some criteria have been established for evaluating hydrocarbon generation potential of organic matter in coal measures in China (Huang and Xiong 1996; Chen et al. 1997; Wang 1998). The criteria from Huang and Xiong (1996) and Wang (1998) for the assessment of hydrocarbon-generating potential of coal-bearing strata are based mainly on two Rock–Eval parameters: TOC and hydrocarbon generative potential ($S_1 + S_2$). However, Chen et al. (1997) found that a plot of HI versus hydrocarbon generative potential ($S_1 + S_2$) is more effective for describing coal-bearing source rock. The criteria from Huang and Xiong (1996) and Wang (1998) are based only on a small number of samples and study areas, while the criteria from Chen et al. (1997) are based on over 23,000 rock samples from coal measure strata in northwestern China. Therefore, the standard established by Chen et al. (1997), which is probably more accurate for evaluating hydrocarbon-generating potential in coal-bearing strata and has been widely accepted (Jiang

Table 1 Rock–Eval data for the K_1d_1 member

Well	Depth (m)	Formation	Lithology	TOC	S_1	S_1/TOC	S_2	$S_1 + S_2$	HI	OI	T_{max}
He-1	1258	K_1d_1	Mudstone	3.90	0.10	0.03	3.68	3.78	94.29	23.32	434
He-1	1261.3	K_1d_1	Mudstone	3.81	0.08	0.02	2.81	2.89	73.79	29.41	436
He-1	1263.5	K_1d_1	Mudstone	3.63	0.11	0.03	3.42	3.53	94.24	31.41	435
He-1	1265.6	K_1d_1	Mudstone	4.27	0.10	0.02	4.13	4.23	96.65	36.51	430
He-1	1635.3	K_1d_1	Mudstone	2.67	0.31	0.12	7.20	7.51	269.87	10.49	431
He-1	1637.7	K_1d_1	Mudstone	2.43	0.47	0.19	11.47	11.94	472.99	11.55	434
He-1	1640.3	K_1d_1	Mudstone	2.88	0.29	0.10	10.16	10.45	352.78	10.42	435
He-1	1736	K_1d_1	Mudstone	1.96	0.21	0.11	5.95	6.16	303.57	87.24	440
He-1	1739.8	K_1d_1	Mudstone	2.36	0.28	0.12	7.04	7.33	298.05	46.99	439
He-6	1357.4	K_1d_1	Mudstone	2.88	0.17	0.06	3.06	3.23	106.15	1520.67	442
He-6	1349.1	K_1d_1	Mudstone	1.79	0.07	0.04	1.84	1.91	102.91	827.42	439
He-6	1350.1	K_1d_1	Mudstone	1.53	0.05	0.03	1.49	1.54	97.20	118.36	440
He-6	1352.4	K_1d_1	Mudstone	1.67	0.06	0.04	1.22	1.28	72.97	225.99	448
He-6	1353.1	K_1d_1	Mudstone	1.91	0.07	0.04	1.90	1.97	99.69	8.69	436
He-6	1354.3	K_1d_1	Mudstone	1.48	0.08	0.05	1.84	1.92	123.99	8.20	441
He-6	1355.1	K_1d_1	Mudstone	1.77	0.06	0.03	1.54	1.60	86.91	2193.58	442
He-X1	2083.8	K_1d_1	Mudstone	1.89	0.28	0.15	4.21	4.49	222.56	1092.27	447
He-X1	2084.3	K_1d_1	Mudstone	2.18	0.33	0.15	5.58	5.91	255.55	602.94	446
He-X1	2084.8	K_1d_1	Mudstone	1.81	0.26	0.14	4.86	5.12	268.28	613.99	446
He-X1	2085.3	K_1d_1	Mudstone	1.73	0.26	0.15	3.55	3.81	204.73	1200.78	442
He-X1	2085.7	K_1d_1	Mudstone	1.61	0.23	0.14	3.37	3.60	209.36	1262.23	445
He-X1	2086.2	K_1d_1	Mudstone	2.18	0.34	0.16	5.70	6.04	261.54	2331.94	445
He-X1	2086.7	K_1d_1	Mudstone	2.29	0.36	0.16	7.02	7.38	305.90	289.09	447
He-X1	2087.2	K_1d_1	Mudstone	1.46	0.18	0.12	2.59	2.77	176.91	2842.32	439
He-X1	2087.6	K_1d_1	Mudstone	1.69	0.24	0.14	3.74	3.98	221.26	2296.84	446
He-X1	2088	K_1d_1	Mudstone	2.26	0.35	0.15	6.80	7.14	301.09	531.84	446
He-X1	2088.4	K_1d_1	Mudstone	1.69	0.23	0.14	4.19	4.41	246.96	209.90	446
He-X1	2089.2	K_1d_1	Mudstone	1.99	0.28	0.14	5.62	5.90	281.89	11.97	447
He-X1	2090.2	K_1d_1	Mudstone	2.20	0.33	0.15	6.56	6.89	298.44	779.19	446
He-X1	2090.4	K_1d_1	Mudstone	1.61	0.21	0.13	4.07	4.28	252.11	842.11	447
He-X1	2090.9	K_1d_1	Mudstone	1.81	0.22	0.12	4.78	5.00	264.16	281.72	448
He-X1	2091.2	K_1d_1	Mudstone	1.88	0.22	0.12	4.75	4.97	252.00	12.38	447
He-X1	2091.5	K_1d_1	Mudstone	1.82	0.21	0.12	4.72	4.93	259.42	126.98	447
Hui-1	1170	K_1d_1	Mudstone	2.11	0.09	0.04	1.37	1.46	64.93	433.63	418
Hui-1	1230	K_1d_1	Mudstone	2.61	0.11	0.04	1.85	1.96	70.77	15.91	420
Hui-1	1340	K_1d_1	Mudstone	1.73	0.11	0.06	2.53	2.64	146.50	144.58	416
He-10	1752	K_1d_1	Mudstone	1.96	0.08	0.04	3.02	3.09	154.16	10.99	438
He-10	1816	K_1d_1	Mudstone	2.62	0.11	0.04	3.27	3.38	124.86	8.33	439
He-12	1868.5	K_1d_1	Mudstone	2.01	0.24	0.12	5.07	5.31	252.14	201.82	440
He-12	1871.4	K_1d_1	Mudstone	2.03	0.23	0.11	4.59	4.82	226.49	11.95	440
He-12	1872.8	K_1d_1	Mudstone	2.53	0.42	0.17	8.13	8.55	321.23	8.60	440
He-12	1875.2	K_1d_1	Mudstone	3.17	0.36	0.11	10.19	10.56	321.20	7.97	441
He-15	1920	K_1d_1	Mudstone	1.73	0.10	0.06	2.60	2.71	150.72	158.29	445
He-15	1940	K_1d_1	Mudstone	1.84	0.01	0.01	2.52	2.52	136.91	624.33	442
He-15	1960	K_1d_1	Mudstone	2.44	0.08	0.03	3.34	3.42	136.80	211.35	437

The units of the Rock–Eval pyrolysis parameters and indices: TOC: wt%; T_{max}: °C; S_1: mg HC/g rock; S_1/TOC: mg HC/g TOC; S_2: mg HC/g rock; S_3: mg CO_2/g rock; HI: mg HC/g TOC; OI: mg CO_2/g TOC

Table 2 Rock–Eval data for the K_1n_2 member

Well	Depth (m)	Formation	Lithology	TOC	S_1	S_1/TOC	S_2	$S_1 + S_2$	HI	OI	T_{max}
He-1	1785.7	K_1n_2	Mudstone	2.46	0.28	0.11	4.30	4.58	174.65	0.00	432
He-1	1827.3	K_1n_2	Mudstone	2.69	0.41	0.15	8.37	8.78	310.92	7.80	435
He-1	1829.3	K_1n_2	Mudstone	2.39	0.30	0.13	5.55	5.85	232.70	17.19	436
He-1	1831.4	K_1n_2	Mudstone	2.45	0.36	0.15	6.57	6.93	268.16	1.22	440
He-1	1938	K_1n_2	Mudstone	3.27	0.51	0.16	5.99	6.50	183.29	0.00	442
He-1	2024	K_1n_2	Mudstone	6.95	3.15	0.45	18.82	21.97	270.99	0.00	437
He-9	1895	K_1n_2	Mudstone	2.16	0.03	0.01	0.18	0.21	8.34	1058.38	472
He-9	1900	K_1n_2	Mudstone	3.97	0.10	0.03	2.46	2.56	62.04	1642.40	437
He-9	1905	K_1n_2	Mudstone	2.69	0.11	0.04	2.08	2.19	77.27	337.30	440
He-9	1910	K_1n_2	Mudstone	2.51	0.33	0.13	3.35	3.67	133.57	1151.28	444
He-9	1915	K_1n_2	Mudstone	1.43	0.25	0.17	2.18	2.43	152.45	967.99	446
He-9	1920	K_1n_2	Mudstone	1.19	0.02	0.02	0.23	0.26	19.38	1539.65	450
He-9	1925	K_1n_2	Mudstone	1.08	0.07	0.06	1.13	1.20	104.63	19.16	442
He-9	1930	K_1n_2	Mudstone	1.71	0.04	0.02	0.66	0.69	38.60	409.36	439
He-9	1935	K_1n_2	Mudstone	7.29	0.25	0.03	10.02	10.27	137.39	6.39	442
He-9	1940	K_1n_2	Mudstone	1.35	0.19	0.14	1.78	1.98	131.95	24.12	446
He-9	1945	K_1n_2	Mudstone	0.65	0.07	0.11	0.72	0.79	110.68	4.16	448
He-9	1950	K_1n_2	Mudstone	1.71	0.12	0.07	2.31	2.42	135.01	0.50	449
He-9	1955	K_1n_2	Mudstone	1.48	0.17	0.11	2.20	2.37	149.15	4.19	449
He-9	1965	K_1n_2	Mudstone	2.31	0.33	0.14	4.10	4.43	177.41	1279.30	449
He-9	1970	K_1n_2	Mudstone	2.22	0.10	0.05	2.05	2.15	92.51	1032.03	444
He-9	1975	K_1n_2	Mudstone	0.78	0.05	0.06	0.67	0.72	86.34	1342.87	449
He-9	1980	K_1n_2	Mudstone	1.61	0.23	0.14	2.75	2.98	170.60	110.05	449
He-9	1985	K_1n_2	Mudstone	1.49	0.20	0.13	1.89	2.09	126.51	96.50	443
He-9	1990	K_1n_2	Mudstone	1.69	0.23	0.14	2.42	2.65	143.20	146.59	449
He-10	1857	K_1n_2	Mudstone	2.00	0.08	0.04	2.38	2.45	118.76	144.44	436
He-10	1873	K_1n_2	Mudstone	2.05	0.06	0.03	2.52	2.58	123.11	122.81	439
He-10	1889	K_1n_2	Mudstone	5.88	1.02	0.17	11.50	12.51	195.51	26.88	436
He-10	1905	K_1n_2	Mudstone	2.27	0.14	0.06	2.27	2.41	99.82	1871.76	439
He-10	2050	K_1n_2	Mudstone	2.84	0.36	0.13	4.07	4.43	143.16	1631.05	441
He-10	2065	K_1n_2	Mudstone	2.60	0.42	0.16	4.18	4.60	160.89	688.49	447
He-10	2109	K_1n_2	Mudstone	4.18	0.68	0.16	6.89	7.57	164.99	543.73	447
He-10	2308	K_1n_2	Mudstone	3.21	0.42	0.13	4.58	5.00	142.90	3.31	451
He-10	2328	K_1n_2	Mudstone	9.08	1.94	0.21	18.45	20.39	203.24	325.40	461
He-10	2348	K_1n_2	Mudstone	5.47	0.48	0.09	7.59	8.07	138.71	685.92	443
He-15	2312	K_1n_2	Mudstone	4.11	0.90	0.22	4.39	5.29	106.65	1122.42	463
He-15	2312.2	K_1n_2	Mudstone	6.03	1.73	0.29	8.60	10.33	142.67	1163.77	464
He-15	2312.6	K_1n_2	Mudstone	0.83	0.05	0.06	0.37	0.42	44.58	1532.13	479
He-15	2416	K_1n_2	Mudstone	4.42	2.05	0.46	5.47	7.52	123.59	1837.28	468
He-X1	2295.2	K_1n_2	Mudstone	2.45	0.44	0.18	4.05	4.49	165.01	11.99	449
He-X1	2295.7	K_1n_2	Mudstone	2.32	0.39	0.17	3.86	4.25	166.11	18.44	450
He-X1	2296.2	K_1n_2	Mudstone	2.64	0.48	0.18	4.56	5.04	172.75	14.46	450
He-X1	2296.6	K_1n_2	Mudstone	2.37	0.45	0.19	3.58	4.03	151.33	27.60	450
He-X1	2297	K_1n_2	Mudstone	2.26	0.46	0.20	3.18	3.64	140.56	51.96	448
He-X1	2297.6	K_1n_2	Mudstone	2.18	0.39	0.18	3.99	4.38	182.74	28.97	450
He-X1	2298	K_1n_2	Mudstone	2.18	0.38	0.17	4.20	4.58	192.51	19.42	449
He-X1	2298.5	K_1n_2	Mudstone	2.28	0.41	0.18	3.69	4.10	161.84	259.04	450
He-X1	2299	K_1n_2	Mudstone	2.25	0.46	0.20	3.03	3.49	135.14	59.20	445

Table 2 continued

Well	Depth (m)	Formation	Lithology	TOC	S_1	S_1/TOC	S_2	S_1+S_2	HI	OI	T_{max}
He-X1	2299.9	K_1n_2	Mudstone	2.55	0.50	0.20	4.06	4.56	159.47	37.00	450
He-1	1833.7	K_1n_2	Coal	64.15	31.92	0.50	239.46	271.38	373.28	3.97	430
He-1	1835.3	K_1n_2	Coal	55.06	8.07	0.15	92.85	100.92	168.63	2.86	435
He-6	1485.9	K_1n_2	Coal	34.69	4.05	0.12	89.63	93.68	258.37	2.35	417
He-6	1489.3	K_1n_2	Coal	72.57	9.58	0.13	141.41	150.99	194.86	8.79	420
He-6	1491.6	K_1n_2	Coal	60.61	7.00	0.12	97.80	104.80	161.36	9.40	440
He-6	1492.4	K_1n_2	Coal	53.70	5.32	0.10	127.02	132.34	236.54	11.47	431
He-6	1492.7	K_1n_2	Coal	32.72	4.76	0.15	98.12	102.88	299.84	9.39	427
He-6	1492.7	K_1n_2	Coal	32.72	4.76	0.15	98.12	102.88	299.84	10.11	427
He-8	2524.8	K_1n_2	Coal	32.82	7.55	0.23	60.75	68.30	185.10	10.11	460
He-9	1632.9	K_1n_2	Coal	49.54	21.72	0.44	186.09	207.81	375.64	4.91	427
He-9	1635.8	K_1n_2	Coal	23.00	2.98	0.13	54.35	57.33	236.30	4.43	426
He-X1	2275	K_1n_2	Coal	64.98	13.07	0.20	152.42	165.49	234.57	2.10	437
He-X1	2283	K_1n_2	Coal	73.30	16.53	0.23	228.49	245.02	311.71	9.93	440

The units of the Rock-Eval pyrolysis parameters and indices: TOC: wt%; T_{max}: °C; S_1: mg HC/g rock; S_1/TOC: mg HC/g TOC; S_2: mg HC/g rock; S_3: mg CO_2/g rock; HI: mg HC/g TOC; OI: mg CO_2/g TOC

et al. 2014; Meng et al. 2014; Song et al. 2015; Zhang et al. 2016), was used in this study. These data indicate that the mudstone samples from the K_1d_1 and K_1n_2 members are fair to good source rocks, while the mudstone samples from the K_1n_1 member have poor source rock characteristics (Figs. 3a–c; Chen et al. 1997).

Based on the analysis of a large number of coal samples in China, Chen et al. (1997) found that a combination of HI and $S_1 + S_2$ can better estimate the hydrocarbon-generating potential of coal. The hydrocarbon generative potential of the coal samples from the K_1n_1 and K_1n_2 members ranged from 12.90 to 81.08 mg HC/g TOC (mean = 43.45 mg HC/g TOC) and from 57.33 to 271.38 mg HC/g TOC (mean = 138.76 mg HC/g TOC), respectively; HI values are in the range of 50.83 to 186.91 mg HC/g TOC (mean = 136.61 mg HC/g TOC) and 161.36 to 375.64 mg HC/g TOC (mean = 256.62 mg HC/g TOC), respectively (Tables 2 and 3). These data indicate that the K_1n_1 coal members have poor hydrocarbon potential, and the K_1n_2 coal member has poor to good hydrocarbon potential (Fig. 3d). The cross plot of HI versus T_{max} (Fig. 4) indicates that the Huhehu source rocks are primarily type II_2 kerogen, with some samples falling in the zone of type II_1 and III kerogen. The Rock–Eval parameters S_1 and TOC are useful in distinguishing between the indigenous and nonindigenous organic matter present in the studied source rock samples (Hunt 1996). A migration index (S_1/TOC) < 1.5 indicates that samples have not been affected by migrated hydrocarbon (e.g., Mashhadi et al. 2015). All the studied source rocks exhibit S_1/TOC ratios < 1.5, indicating that the studied samples were not contaminated by migrated hydrocarbon.

4.2 Molecular characteristics of source rocks

The gas chromatogram shows front-end biased distribution and enrichment of low molecular compounds, typically at n-C_{17} to n-C_{23} (Figs. 5 and 6). No apparent odd-over-even predominance was observed other than in coal. A low Pr/Ph ratio (< 1) indicates an anoxic depositional environment, whereas a higher Pr/Ph ratio (> 1) indicates oxic depositional conditions (Didyk et al. 1978). Additionally, extremely high values of the Pr/Ph ratio (> 3) are believed to be associated with terrigenous organic matter inputs under oxic depositional settings (Peters et al. 2005). The Pr/Ph ratios for the source rock from the K_1d_1, K_1n_1, and K_1n_2 members are in the range of 1.25 to 2.39 (mean = 1.77, 16 samples), 2.24 to 3.24 (mean = 2.74, 2 samples), and 1.43 to 4.07 (mean = 2.52, 13 samples) (Table 4), respectively, suggesting oxic depositional conditions for these source rock members. Furthermore, the mean values of Pr/Ph increase as follows: $K_1d_1 < K_1n_2 < K_1n_1$ members, probably indicating relatively oxic depositional conditions.

Sterane mass chromatograms (m/z 217) of the representative source rocks are shown in Figs. 5 and 6. The relative abundances of C_{27}, C_{28}, and C_{29} steranes for the source rocks are in the range of 12.27%–41.51%, 8.16%–24.56%, and 41.98%–74.11%, respectively (Table 4). Previous work observed that C_{27} sterols (steranes) dominate in marine organic matter, while C_{29} sterols (steranes) dominate in terrigenous organic matter (Huang and Meinschein 1979). Our data suggest a dominant contribution of terrigenous organic matter input (Fig. 7). In addition, sterane/hopane ratios for the source rocks range from 0.07

Table 3 Rock-Eval data for the K_1n_1 member

Well	Depth (m)	Formation	Lithology	TOC	S_1	S_1/TOC	S_2	$S_1 + S_2$	HI	OI	T_{max}
He-10	2368	K_1n_1	Mudstone	2.99	0.32	0.11	3.24	3.56	108.43	41.83	450
He-10	2388	K_1n_1	Mudstone	1.09	0.10	0.09	1.32	1.42	120.77	46.66	456
He-10	2409	K_1n_1	Mudstone	1.39	0.18	0.13	1.52	1.69	109.35	620.14	461
He-10	2428	K_1n_1	Mudstone	5.20	0.67	0.13	8.16	8.84	156.92	16.54	452
He-10	2448	K_1n_1	Mudstone	2.81	0.33	0.12	3.98	4.30	141.74	18.16	456
He-10	2472	K_1n_1	Mudstone	3.92	0.68	0.17	6.16	6.83	156.98	16.06	453
He-10	2492	K_1n_1	Mudstone	1.12	0.06	0.05	0.94	1.00	84.15	49.24	456
He-10	2512	K_1n_1	Mudstone	1.94	0.34	0.18	2.52	2.85	130.10	81.05	441
He-10	2553	K_1n_1	Mudstone	3.58	0.70	0.20	6.26	6.96	175.01	14.54	454
He-10	2572	K_1n_1	Mudstone	1.43	0.34	0.24	2.04	2.38	142.56	29.35	458
He-8	3353	K_1n_1	Mudstone	0.62	0.01	0.02	0.16	0.17	25.88	82.48	498
He-8	3373	K_1n_1	Mudstone	9.33	0.31	0.03	4.07	4.38	43.62	14.36	502
He-8	3391	K_1n_1	Mudstone	9.80	0.90	0.09	8.03	8.93	81.92	7.35	486
He-8	3414	K_1n_1	Mudstone	1.08	0.04	0.04	0.35	0.39	32.32	93.26	480
He-8	3425	K_1n_1	Mudstone	0.45	0.01	0.02	0.19	0.20	42.44	808.58	461
He-8	3445	K_1n_1	Mudstone	4.53	0.35	0.08	4.48	4.83	99.01	303.87	447
He-8	3458	K_1n_1	Mudstone	1.42	0.09	0.06	1.09	1.18	76.76	452.82	449
He-9	2047	K_1n_1	Mudstone	3.02	0.16	0.05	2.58	2.73	85.37	65.52	447
He-9	2048	K_1n_1	Mudstone	0.98	0.06	0.06	0.83	0.89	84.55	113.07	445
He-9	2050	K_1n_1	Mudstone	2.22	0.20	0.09	2.88	3.09	129.91	56.38	448
He-9	2052	K_1n_1	Mudstone	1.89	0.21	0.11	2.37	2.58	125.33	615.55	449
He-9	2054	K_1n_1	Mudstone	1.19	0.13	0.11	1.16	1.28	97.73	131.42	450
He-9	2056	K_1n_1	Mudstone	2.41	0.18	0.07	2.23	2.40	92.61	696.43	447
He-9	2058	K_1n_1	Mudstone	1.14	0.11	0.10	1.34	1.45	117.13	86.54	449
He-9	2060	K_1n_1	Mudstone	0.53	0.06	0.11	0.59	0.66	110.69	724.20	446
He-9	2062	K_1n_1	Mudstone	2.79	0.29	0.10	3.23	3.52	115.90	76.43	448
He-9	2064	K_1n_1	Mudstone	1.29	0.13	0.10	1.73	1.86	134.42	102.56	449
He-9	2066	K_1n_1	Mudstone	1.35	0.13	0.10	1.72	1.86	127.50	3575.98	444
He-9	2068	K_1n_1	Mudstone	2.73	0.30	0.11	3.37	3.67	123.44	1369.96	443
He-9	2070	K_1n_1	Mudstone	1.45	0.19	0.13	2.20	2.39	151.31	756.53	451
He-9	2072	K_1n_1	Mudstone	1.52	0.08	0.05	1.67	1.75	109.65	1192.38	441
He-9	2074	K_1n_1	Mudstone	0.73	0.04	0.05	0.71	0.75	97.80	154.27	448
He-9	2076	K_1n_1	Mudstone	1.43	0.19	0.13	1.97	2.16	137.86	548.64	447
He-9	2078	K_1n_1	Mudstone	0.50	0.06	0.12	0.53	0.60	105.01	828.21	450
He-9	2080	K_1n_1	Mudstone	1.27	0.12	0.09	1.42	1.54	111.72	567.27	446
He-9	2082	K_1n_1	Mudstone	0.64	0.10	0.16	0.60	0.70	93.72	745.08	450
He-9	2084	K_1n_1	Mudstone	1.57	0.38	0.24	2.62	3.00	167.09	47.83	449
He-9	2086	K_1n_1	Mudstone	1.33	0.22	0.17	1.72	1.94	129.23	174.31	448
He-9	2088	K_1n_1	Mudstone	1.24	0.31	0.25	2.44	2.75	196.30	67.58	450
He-9	2090	K_1n_1	Mudstone	0.81	0.12	0.15	1.03	1.15	126.72	182.09	451
He-9	2092	K_1n_1	Mudstone	1.60	0.18	0.11	1.91	2.09	119.67	904.76	447
He-9	2094	K_1n_1	Mudstone	0.73	0.12	0.16	0.71	0.83	97.72	8867.33	452
He-9	2096	K_1n_1	Mudstone	2.14	0.33	0.15	2.39	2.73	111.94	705.39	449
He-9	2098	K_1n_1	Mudstone	1.51	0.26	0.17	2.24	2.50	148.05	1308.00	449
He-9	2100	K_1n_1	Mudstone	0.82	0.08	0.10	0.90	0.98	110.06	2151.16	448
He-9	2102	K_1n_1	Mudstone	1.04	0.08	0.08	1.16	1.24	111.11	2192.53	444
He-9	2104	K_1n_1	Mudstone	1.82	0.21	0.12	2.22	2.43	121.78	414.70	440
He-X1	3063.8	K_1n_1	Mudstone	0.57	0.02	0.04	0.14	0.16	25.12	26.88	502

Table 3 continued

Well	Depth (m)	Formation	Lithology	TOC	S_1	S_1/TOC	S_2	$S_1 + S_2$	HI	OI	T_{max}
He-X1	3064.4	K_1n_1	Mudstone	0.43	0.01	0.02	0.11	0.12	26.28	26.97	499
He-X1	3065	K_1n_1	Mudstone	0.85	0.04	0.05	0.25	0.28	29.10	17.32	501
He-X1	3065.4	K_1n_1	Mudstone	0.30	0.00	0.00	0.06	0.06	18.64	57.24	498
He-X1	3065.9	K_1n_1	Mudstone	0.17	0.00	0.00	0.02	0.02	12.08	130.43	495
He-X1	3066.4	K_1n_1	Mudstone	0.16	0.00	0.00	0.02	0.02	10.32	130.46	495
He-X1	3067.3	K_1n_1	Mudstone	0.81	0.03	0.04	0.22	0.25	26.88	23.55	500
He-X1	3128.2	K_1n_1	Mudstone	0.39	0.01	0.03	0.07	0.07	16.81	53.54	500
He-X1	3129.1	K_1n_1	Mudstone	0.58	0.03	0.05	0.13	0.16	21.98	30.28	504
He-X1	3129.5	K_1n_1	Mudstone	0.19	0.00	0.00	0.03	0.03	14.56	95.68	502
He-X1	3130.4	K_1n_1	Mudstone	0.28	0.01	0.04	0.04	0.04	13.78	67.11	502
He-X1	3130.8	K_1n_1	Mudstone	0.78	0.05	0.06	0.14	0.19	17.74	23.48	500
He-X1	3131.1	K_1n_1	Mudstone	0.86	0.04	0.05	0.15	0.19	17.64	20.31	501
He-X1	3131.6	K_1n_1	Mudstone	1.32	0.13	0.10	0.39	0.52	29.29	11.02	500
He-10	2532	K_1n_1	Coal	12.11	1.60	0.13	21.96	23.56	181.34	4.74	457
He-X1	3070	K_1n_1	Coal	40.57	4.59	0.11	51.67	56.26	127.37	5.62	442
He-X1	3080	K_1n_1	Coal	23.36	1.02	0.04	11.88	12.90	50.83	0.00	445
He-X1	3160	K_1n_1	Coal	38.83	8.50	0.22	72.58	81.08	186.91	9.54	455

The units of the Rock-Eval pyrolysis parameters and indices: TOC: wt%; T_{max}: °C; S_1: mg HC/g rock; S_1/TOC: mg HC/g TOC; S_2: mg HC/g rock; S_3: mg CO_2/g rock; HI: mg HC/g TOC; OI: mg CO_2/g TOC

to 0.54, indicative of terrigenous or microbially reworked organic matter (Tissot and Welte 1984).

Terpane mass chromatograms (m/z 191) of the representative source rocks are characterized by a high abundance of pentacyclic terpanes relative to tricyclic terpanes (Figs. 5 and 6), consistent with coal-bearing source rocks in northwestern China (J Chen et al. 1998). The C_{35}/C_{34} ratios for the source rocks range from 0.19 to 0.39, indicating oxic depositional conditions (Peters and Moldowan 1991). The gammacerane/C_{31}R ratios in the source rocks are in the range of 0.01 to 0.23, indicating a lack of stratification because a high gammacerane/C_{31}R ratio is usually expected both with stratification and with reducing depositional conditions (Fu et al. 1986; Sinninghe Damsté et al. 1995).

4.3 Maturity of source rocks

To evaluate the thermal maturity of the source rocks, several maturity indicators, including Rock–Eval pyrolysis and biomarker parameters were used. The Rock–Eval pyrolysis parameter, T_{max}, preferred by type II/III organic matter (Tissot et al. 1987), is a reliable index for evaluating thermal maturity of source rocks (Tissot and Welte 1984). Based on T_{max} values in the source rock members (Peters 1986), the K_1d_1 mudstone member is at immature to peak stage, ranging from 416 to 448 °C, and the K_1n_2 mudstone member is at early to late stage, ranging from 432 to 479 °C. It is noteworthy that the K_1n_1 mudstone member has the highest maturity level, while coals from the K_1n_1 and K_1n_2 members are mostly at an immature or early mature stage (Peters 1986). In general, the thermal maturity of the source rock members increase as follows: $K_1d_1 < K_1n_2 < K_1n_1$ members (Tables 1, 2, 3).

With increasing maturity, three biomarker ratios—C_{32} homohopanes 22S/(22S + 22R), C_{29} steranes 20S/(20R + 20S), and C_{29} ββ/(αα + ββ)—increase from 0 to approximately 0.6, 0–0.5, and 0–0.7, respectively (Seifert and Moldowan 1980, 1986). The values of C_{32} homohopane 22S/(22S + 22R) ratios for the Huhehu source rocks are in the range of 0.57–0.61 (Table 4), indicating that most of the source rocks have reached or even surpassed the oil window. The ratios of C_{29} steranes 20S/(20R + 20S) and C_{29} ββ/(αα + ββ) in the Huhehu source rocks are in the range of 0.20–0.55 and 0.30–0.53 (K_1d_1 member), 0.29–0.62 and 0.41–0.50 (K_1n_2 member), and 0.40 to 0.55 and 0.44 to 0.49 (K_1n_1 member) (Table 4). These data suggest that most of the studied samples are mature, which is consistent with the T_{max} values.

4.4 Oil-oil correlation

When the similarity line was placed at a similarity coefficient value of slightly greater than 0.6, the Huhehu oils were divided into three groups: A, B, and C (Fig. 8). This is consistent with PCA results (Fig. 9).

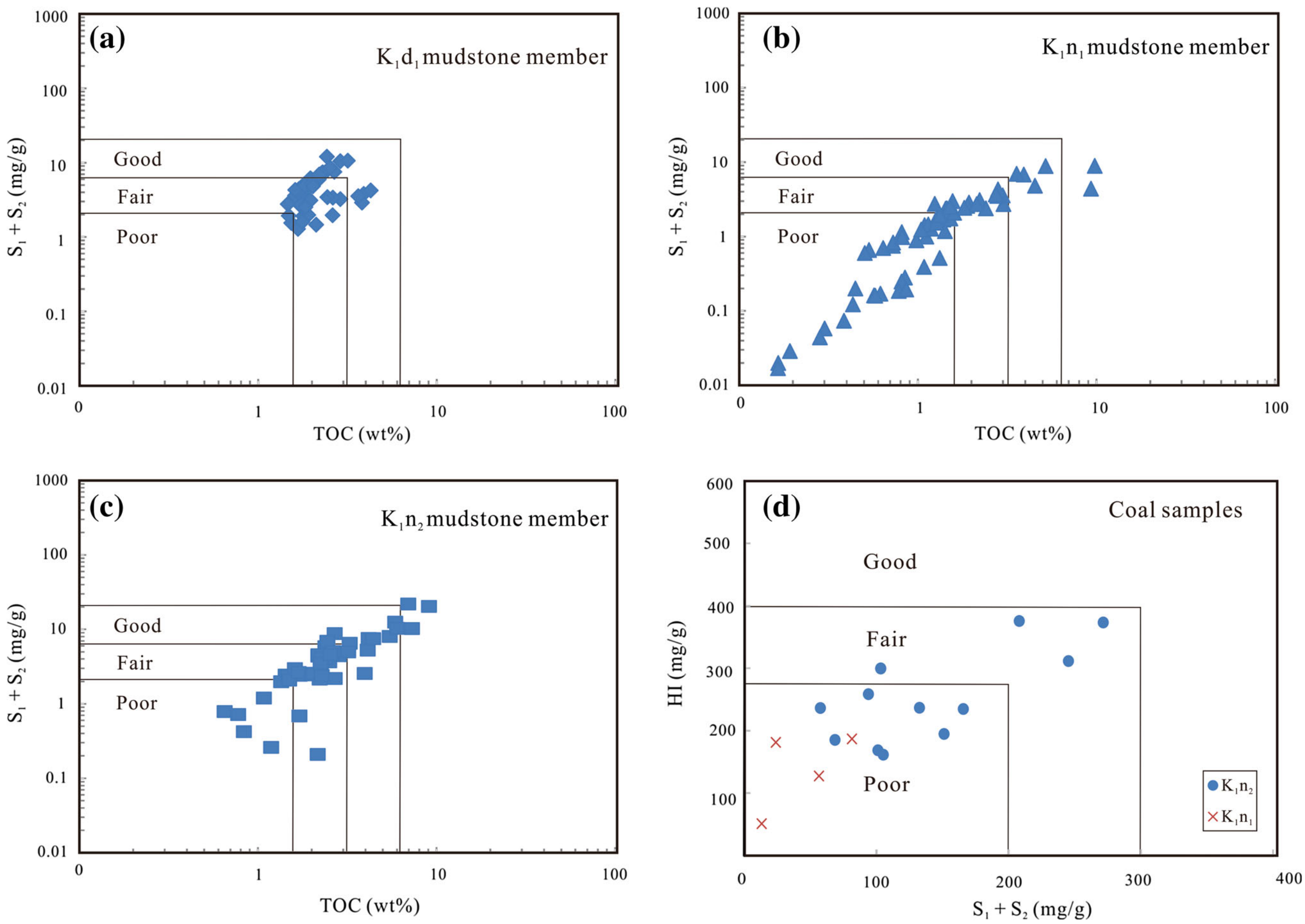

Fig. 3 Plots of the Rock–Eval parameters total organic carbon (TOC) versus $S_1 + S_2$ for source rocks from the K_1d_1, K_1n_2, and K_1n_1 mudstone members (**a**–**c**), and $S_1 + S_2$ vesrus hydrogen index (HI) for source rocks from the K_1n_2 and K_1n_1 coal members (**d**)

4.4.1 Bulk physical properties of crude oils

The physical characteristics of the Huhehu oils have been reported by Lu et al. (2010), and include low density (0.80 g/cm^3), viscosity (1.93 mPa s), freezing point (19 °C), and wax content. These physical properties suggest that the Huhehu oils belong to light crude oil with a low wax content and freezing point (Lu et al. 2010).

4.4.2 Molecular characteristics of crude oil

Gas chromatograms of the representative Huhehu oils are shown in Fig. 10, and the related parameters are listed in Table 4. The *n*-paraffin distribution of the oil has a wide distribution (n-C_{14}–n-C_{35}) with a maximum at about n-C_{19} to n-C_{21}. The high abundance of low-weight molecular *n*-alkanes in the oil suggests a lack of significant biodegradation. Low values of Pr/n-C_{17} and Ph/n-C_{18} ratios also support that the oils are non-biodegraded (Table 4). The plot of Pr/n-C_{17} and Ph/n-C_{18} indicates that the oils can be divided into three families (Fig. 11). The Pr/Ph ratios for the oils are in the range of 1.57–4.53, with an average of 2.94, probably indicating a dominant contribution of terrigenous organic matter input deposited under oxic depositional conditions. The group A oils have moderate values of Pr/Ph, ranging from 2.04 to 3.13. The group B oils display relatively low values of Pr/Ph, ranging from 1.57 to 2.02. The group C oils are characterized by high values of Pr/Ph, ranging from 3.24 to 4.53. These data may indicate that group C oils were deposited under more oxic depositional conditions in comparison with group A and B oils.

Figure 12 shows mass chromatograms of the steranes (m/z 217) of saturated hydrocarbon fractions from the representative Huhehu oils. Although the oils from different categories varied in the distribution of regular steranes (C_{27}–C_{29}), all the oils show high concentrations of C_{29} steranes, which is indicative of a dominant contribution of terrigenous organic matter (Fig. 13). This is consistent with low hopane/sterane ratios, which often infer terrigenous or microbially reworked organic matter input (Tissot and Welte 1984). In comparison with the oils from the two other groups, the group C oils have relatively high

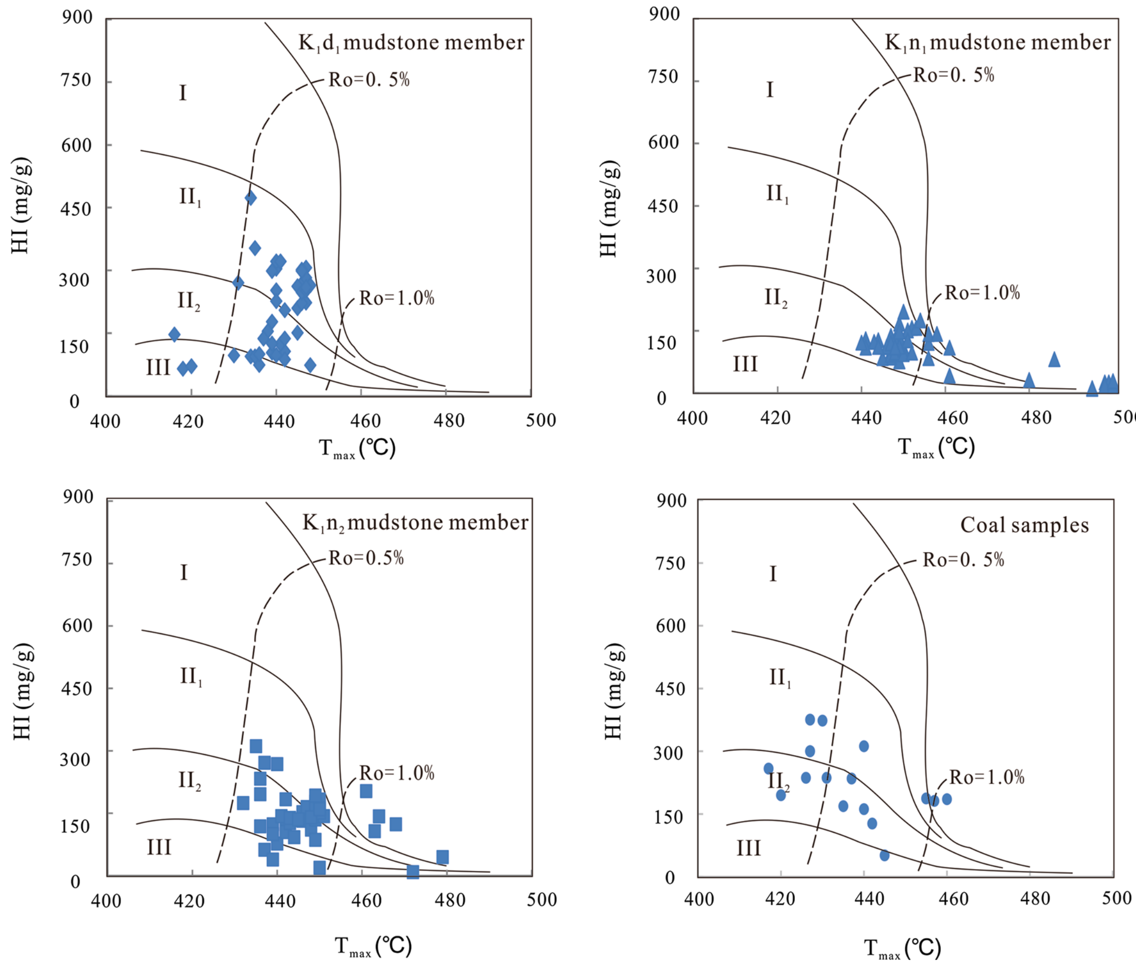

Fig. 4 Plot of hydrogen index (HI) versus T_{max} for the Huhehu source rock showing hydrocarbon generative types

concentrations of C_{29} steranes, probably indicating more terrigenous organic matter input.

Figure 12 displays m/z 191 mass chromatograms of saturated hydrocarbon fractions from the representative Huhehu oils, which clearly display a dominant abundance of pentacyclic terpanes relative to tricyclic terpanes. The low values of C_{35}/C_{34} ratios for the studied crude oils, ranging from 0.05 to 0.45 (Table 4), indicate oxic depositional conditions (Peters and Moldowan 1991). The gammacerane/C_{31}R ratios of the oils indicate a lack of stratification during source rock deposition.

4.4.3 *Thermal maturity of crude oil*

The C_{32} homohopane 22S/(22S + 22R) ratios for the oils are in the range of 0.50–0.60, indicating that the oils have reached equilibrium (Seifert and Moldowan 1980). Group A oils have high ratios of C_{29} steranes 20S/(20R + 20S) and C_{29} $\beta\beta/(\alpha\alpha + \beta\beta)$ (ranging from 0.44 to 0.47 and from 0.45 to 0.53, respectively), indicating that they are mature (Seifert and Moldowan 1986). In comparison, the group C oils have relatively low values of C_{29} steranes 20S/(20R + 20S) and C_{29} $\beta\beta/(\alpha\alpha + \beta\beta)$ (ranging from 0.32 to 0.40 and from 0.32 to 0.42, respectively); and the group B oils have moderate values of C_{29} steranes 20S/(20R + 20S) and C_{29} $\beta\beta/(\alpha\alpha + \beta\beta)$ (0.35–0.43 and 0.43–0.49, respectively). Thermal maturity of the crude oils in all the groups decreases overall in the following order: A > B > C (Fig. 14).

4.5 Oil–source rock correlation

The three-dimensional view of PCA was used to identify the relationship between the oils and the candidate source rocks using range scale preprocessing, Euclidean metric distance, and incremental linkage in Pirouette® (Infometrix, Inc.). The first three components of the PCA (PC1, PC2, and PC3) account for 90% of the total variance in the original dataset. As shown in Fig. 15a, three genetic oil families were determined. Group A oils show strong affinity to the K_1n_2 and K_1n_1 mudstones members. The K_1d_1 mudstone member is related to the group B oils, and

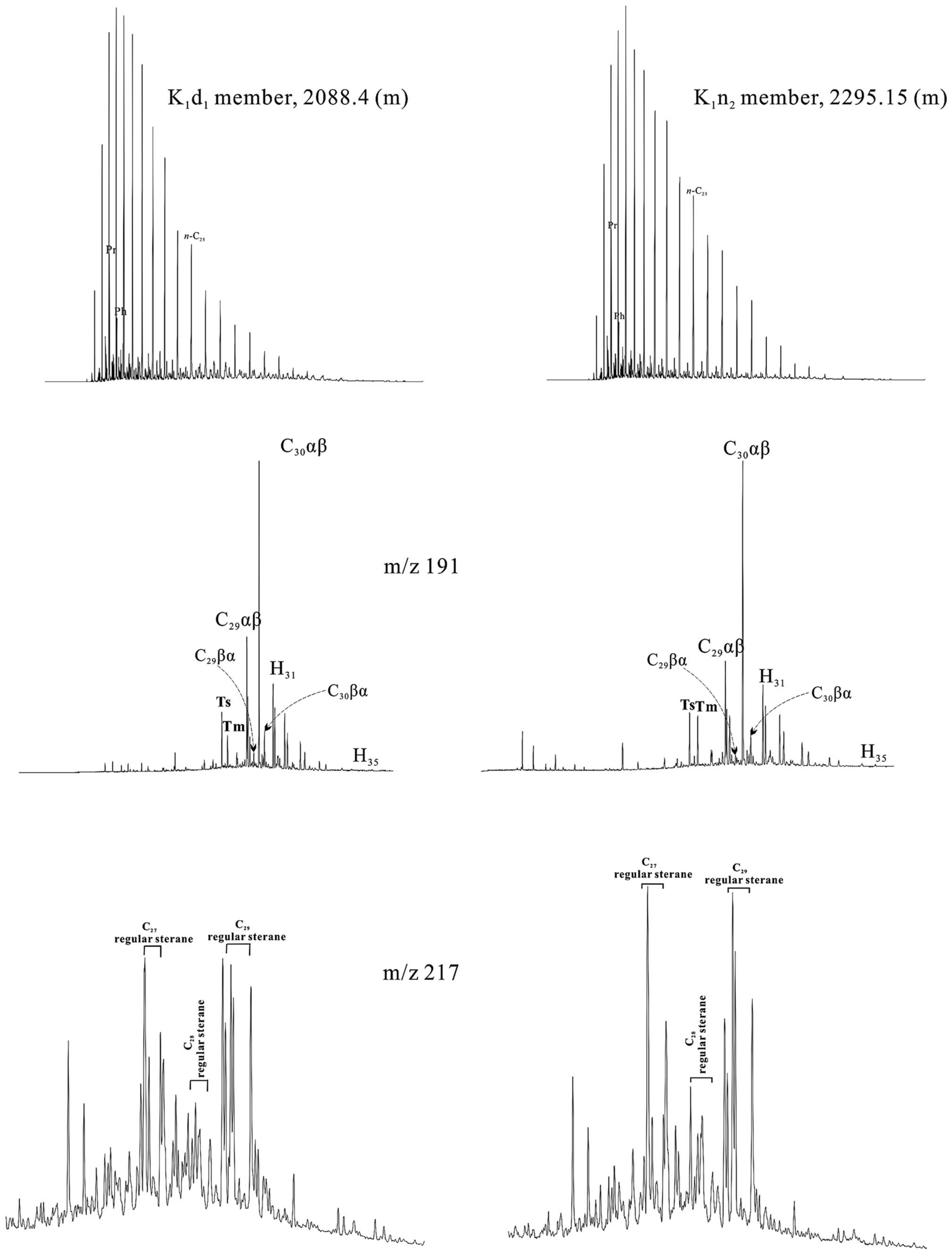

Fig. 5 Representative TIC, hopane (m/z 191), and sterane (m/z 217) mass chromatograms for the source rocks from the K_1d_1 and K_1n_2 members

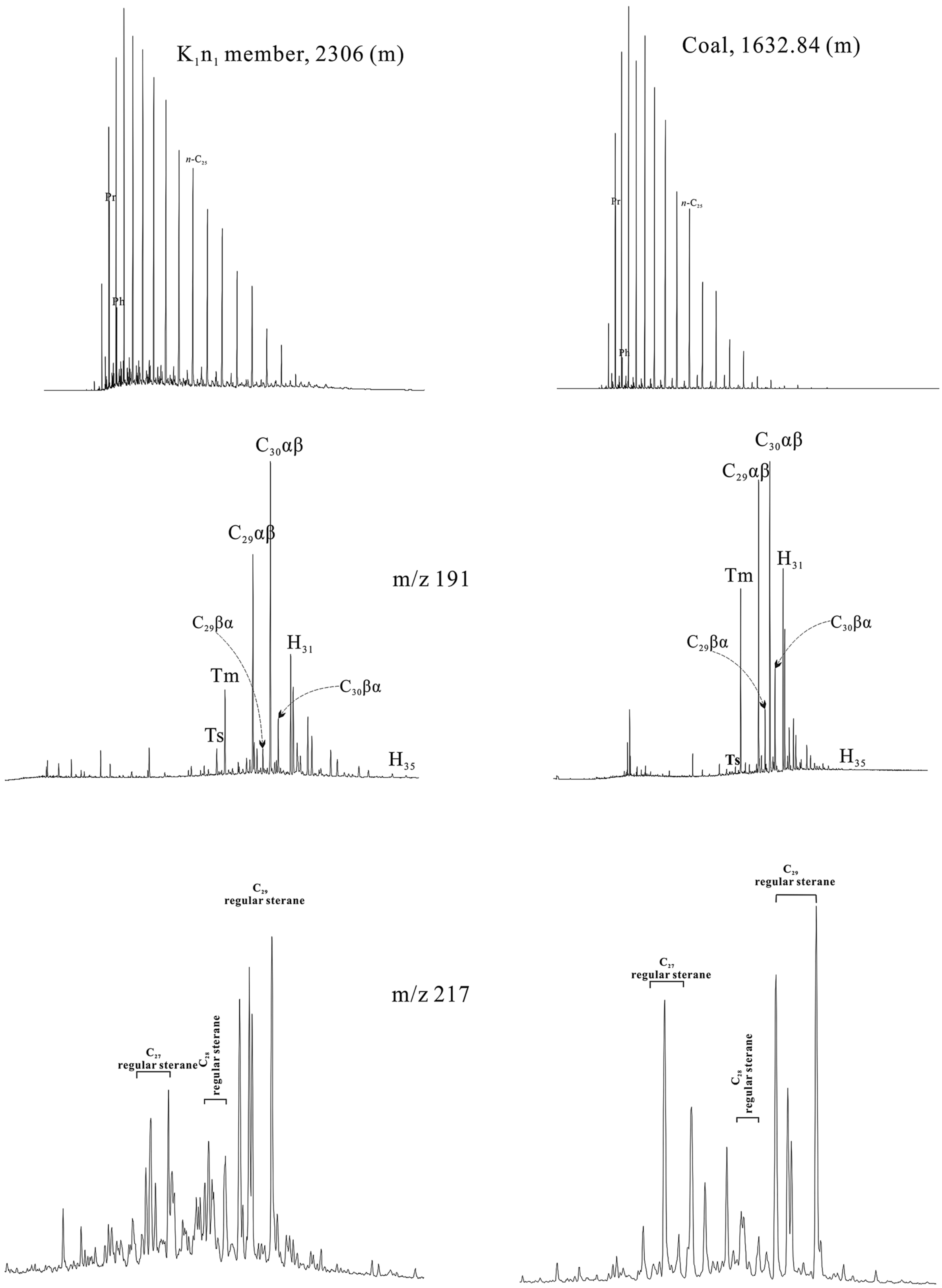

Fig. 6 Representative TIC, hopane (m/z 191), and sterane (m/z 217) mass chromatograms for the source rocks from the K_1n_1 member and coal samples

Table 4 Selected biomarker parameters for the source rock extracts and oils in the Huhehu Sag

Lab no.	Strata	Lithology	well	Depth (m)	R1#	R2	R3	R4#	R5#	R6	R7#	R8#	R9#	R10#	R11#	R12#	R13#	R14	R15
1	K_1d_1	Mudstone	He-1	1736	1.38	0.52	0.22	0.25	0.8	0.59	0.27	0.21	0.04	0.18	39.55	12.54	47.91	0.22	0.35
2	K_1d_1	Mudstone	X1	2083	1.91	0.29	0.11	0.64	0.41	0.58	0.19	0.32	0.15	0.07	33.77	12.1	54.14	0.54	0.53
3	K_1d_1	Mudstone	X1	2084.3	1.99	0.31	0.13	0.63	0.4	0.58	0.18	0.32	0.09	0.07	34.9	11.56	53.54	0.53	0.52
4	K_1d_1	Mudstone	X1	2086.2	2.12	0.35	0.13	0.66	0.41	0.58	0.18	0.33	0.09	0.08	31.64	12.58	55.78	0.52	0.51
5	K_1d_1	Mudstone	X1	2088.4	1.92	0.31	0.12	0.61	0.42	0.58	0.2	0.25	0.06	0.12	32.58	13.35	54.07	0.53	0.5
6	K_1d_1	Mudstone	X1	2090.4	2.18	0.32	0.11	0.62	0.44	0.58	0.19	0.3	0.1	0.08	35.28	11.76	52.96	0.54	0.51
7	K_1d_1	Mudstone	X1	2091.5	2.04	0.31	0.12	0.61	0.44	0.58	0.21	0.28	0.07	0.08	35.25	11.31	53.44	0.53	0.52
8	K_1d_1	Mudstone	He-5	1707.1	1.75	0.54	0.17	0.9	0.78	0.57	0.47	0.22	0.01	0.17	26.09	14.42	59.49	0.2	0.3
9	K_1d_1	Mudstone	He-5	1708.7	1.83	0.59	0.18	0.89	0.79	0.57	0.45	0.2	0.04	0.16	27.19	14.36	58.45	0.2	0.31
10	K_1d_1	Mudstone	He-5	1894	2.39	0.7	0.18	0.25	0.58	0.58	0.26	0.37	0.01	0.22	33.46	24.56	41.98	0.35	0.39
11	K_1d_1	Mudstone	He-5	1920	1.73	0.33	0.12	0.11	0.79	0.58	0.37	0.33	0.05	0.2	31.17	13.97	54.86	0.29	0.45
12	K_1d_1	Mudstone	He-5	1966	1.68	0.46	0.16	0.35	0.64	0.6	0.27	0.33	0.04	0.14	33.46	12.93	53.61	0.37	0.46
13	K_1d_1	Mudstone	He-8	2126.7	1.35	0.34	0.15	0.16	0.62	0.61	0.28	0.26	0.04	0.19	35.18	13.36	51.46	0.55	0.48
14	K_1d_1	Mudstone	He-8	2127.6	1.43	0.32	0.09	0.25	0.59	0.6	0.27	0.31	0.06	0.21	38.03	14.1	47.87	0.53	0.5
15	K_1d_1	Mudstone	He-8	2131.1	1.41	0.29	0.14	0.38	0.5	0.6	0.24	0.33	0.06	0.2	39.4	14.08	46.52	0.53	0.49
16	K_1d_1	Mudstone	He-8	2135.2	1.25	0.23	0.11	0.42	0.47	0.6	0.23	0.32	0.05	0.2	41.51	13.67	44.82	0.55	0.5
17	K_1n_2	Mudstone	X1	2295.2	2.82	0.42	0.11	0.51	0.35	0.58	0.2	0.29	0.09	0.19	33.02	14.37	52.61	0.51	0.46
18	K_1n_2	Mudstone	X1	2297	2.81	0.41	0.11	0.48	0.35	0.58	0.19	0.26	0.07	0.17	29.74	15.07	55.19	0.55	0.49
19	K_1n_2	Mudstone	X1	2299	2.74	0.47	0.12	0.42	0.36	0.59	0.21	0.28	0.1	0.19	30.99	15.29	53.72	0.54	0.48
20	K_1n_2	Mudstone	X1	2309.4	2.08	0.79	0.26	0.39	0.46	0.59	0.18	0.3	0.05	0.3	28.95	13.32	57.73	0.56	0.48
21	K_1n_2	Mudstone	X1	2319.5	2.88	0.47	0.12	0.44	0.39	0.59	0.21	0.28	0.08	0.22	25.45	16.97	57.58	0.53	0.49
22	K_1n_2	Mudstone	He-5	2104	1.53	0.87	0.4	0.22	0.88	0.59	0.29	0.27	0.12	0.3	25.49	15.4	59.1	0.49	0.47
23	K_1n_2	Mudstone	He-5	2016	1.81	1.55	0.32	0.07	1.22	0.6	0.38	0.28	0.08	0.16	21.41	13.02	65.57	0.44	0.46
24	K_1n_2	Mudstone	He-7	2040.9	2.65	0.45	0.13	0.12	0.99	0.59	0.3	0.29	0.11	0.09	24.75	15.09	60.15	0.39	0.48
25	K_1n_2	Mudstone	He-7	2042.1	2.86	0.87	0.16	0.05	1.01	0.6	0.32	0.29	0.04	0.13	25.51	11.54	62.95	0.38	0.49
26	K_1n_2	Mudstone	He-9	1589.4	2.6	0.98	0.22	0.08	1.22	0.57	0.41	0.32	0.02	0.14	24.45	12.94	62.61	0.29	0.41
27	K_1n_2	Mudstone	He-9	2014.1	4.07	0.44	0.07	0.28	0.45	0.59	0.3	0.39	0.05	0.21	22.78	13.76	63.46	0.55	0.5
28	K_1n_2	Mudstone	He-9	2017.1	1.43	0.58	0.14	0.35	0.43	0.58	0.25	0.33	0.1	0.27	29.24	16.04	54.72	0.62	0.5
29	K_1n_2	Mudstone	He-9	2017.6	2.07	1.14	0.17	0.37	0.41	0.59	0.22	0.26	0.07	0.34	23.65	15.53	60.82	0.61	0.5
30	K_1n_1	Mudstone	He-2	1679.5	3.24	0.99	0.2	0.35	0.5	0.6	0.17	0.26	0.08	0.14	33.95	16.22	49.83	0.55	0.49
31	K_1n_1	Mudstone	He-5	2306	2.24	0.82	0.2	0.24	0.62	0.59	0.28	0.33	0.23	0.24	24.38	18.18	57.45	0.4	0.44
32	K_1n_2	coal	He-5	2240.7	3.93	2.52	0.3	0.3	0.46	0.6	0.28	0.29	0.08	0.34	15.08	14.11	70.82	0.35	0.34
33	K_1n_2	coal	He-5	2243.7	3.45	1.96	0.26	0.86	0.47	0.6	0.25	0.28	0.07	0.3	16.07	15.93	68	0.34	0.34
34	K_1n_2	coal	He-9	1632.8	5.17	0.66	0.1	0.95	0.88	0.61	0.45	0.19	0.08	0.25	28.19	13.72	58.09	0.29	0.27
35	K_1n_1	coal	He-5	2237.5	2.46	3.47	0.3	0.26	0.56	0.6	0.3	0.29	0.13	0.45	12.27	13.63	74.11	0.44	0.37
	Group A																		

Table 4 continued

Lab no.	Strata	Lithology	well	Depth (m)	R1#	R2	R3	R4#	R5#	R6	R7#	R8#	R9#	R10#	R11#	R12#	R13#	R14	R15
36	K_1n_1	oil	He-2	1669.00-1649.80	2.04	0.31	0.14	0.56	0.45	0.57	0.17	0.44	0.1	0.34	22.07	16.2	61.73	0.46	0.49
37	K_1n_1	oil	He-2	1669.00-1841.80	2.17	0.22	0.11	0.65	0.48	0.59	0.2	0.3	0.1	0.31	27.93	15.96	56.11	0.44	0.53
38	K_1n_2	oil	He-9	1604.3	2.9	0.35	0.12	0.23	0.72	0.59	0.32	0.36	0.08	0.25	22.92	13.8	63.28	0.45	0.45
39	K_1n_1	oil	He-2	1652.7	3.13	0.43	0.1	0.43	0.47	0.6	0.23	0.44	0.06	0.25	25.97	16.73	57.3	0.47	0.48
	Group B																		
40	K_1n_2	oil	He-2	1550.3	1.67	0.56	0.16	0.85	1.17	0.56	0.38	0.1	0.03	0.15	25.6	24.34	50.06	0.43	0.48
41	K_1n_2	oil	He-2	1550.3	2.02	0.61	0.16	0.85	1.23	0.54	0.37	0.05	0.03	0.11	20.66	27.94	51.4	0.43	0.44
42	K_1n_2	oil	He-2	1550.3	1.78	0.54	0.16	0.83	1.23	0.55	0.4	0.45	0.04	0.13	25.38	23.14	51.48	0.4	0.49
43	K_1n_2	oil	He-2	1550.3	1.57	0.44	0.14	0.85	1.14	0.55	0.37	0.2	0.06	0.11	24.68	21.84	53.48	0.35	0.43
	Group C																		
44	K_1n_2	oil	He-6	1492.6	4.12	2.15	0.29	0.9	0.91	0.56	0.53	0.42	0.04	0.17	13.15	17.14	69.71	0.37	0.4
45	K_1n_2	oil	He-6	1492.6	3.24	2.08	0.31	0.87	0.86	0.5	0.42	0.24	0.04	0.17	11	13.78	75.22	0.32	0.34
46	K_1n_2	oil	He-6	1492.6	4.53	2.24	0.32	0.82	0.91	0.5	0.52	0.12	0.03	0.19	12.69	21.77	65.54	0.36	0.32
47	K_1n_2	oil	He-6	1492.6	3.71	2.19	0.32	0.84	0.88	0.5	0.41	0.42	0.05	0.17	12.49	21.69	65.83	0.34	0.36
48	K_1n_2	oil	He-6	1492.6	3.91	1.85	0.28	0.84	0.85	0.55	0.39	0.17	0.03	0.14	15.61	20.91	63.48	0.33	0.33
49	K_1n_2	oil	He-6	1492.6	3.37	1.73	0.28	0.85	0.87	0.52	0.37	0.07	0.06	0.13	17	16.45	66.55	0.34	0.4
50	K_1n_2	oil	He-6	1492.6	3.93	2.36	0.34	0.86	0.84	0.56	0.36	0.33	0.05	0.15	16.58	21	62.41	0.4	0.42

Those marked parameters with star are used in the cluster analysis, principal component analysis. R1 = pristane/phytane; R2 = pristine/n-C_{17}; R3 = phytane/n-C_{18}; R4 = Ts/(Ts +Tm); R5 = C_{29} hopane/C_{30} hopane; R6 = C_{32} 22S/(22S + 22R) homohopane isomerization; R7 = C_{31} 22R/C_{30} hopane; R8 = C_{35}/C_{34} homohopanes; R9 = gammacerane/C_{31} 22R hopane; R10 = steranes/hopanes; R11 = %C_{27} (e.g., %C_{27} = %C_{27}/(%C_{27}–%C_{29}); R12 = %C_{28}; R13 = %C_{29}; R14 = C_{29} ββ/(αα + ββ); R15 = C_{29} steranes 20S/(20R + 20S). These parameters can be referred to Peters et al. (2005) in detail

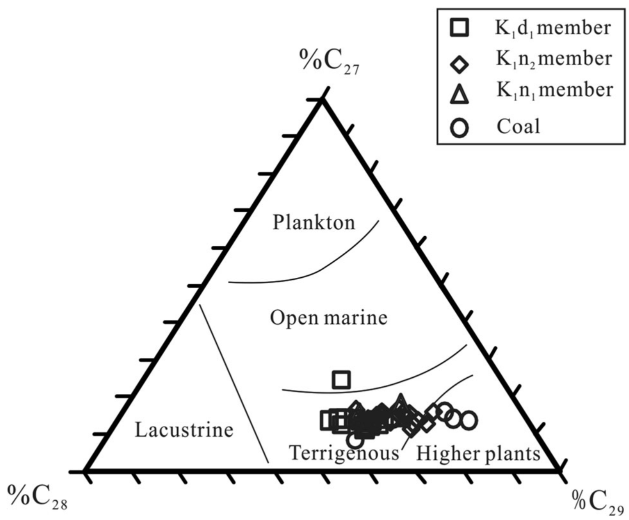

Fig. 7 Ternary diagram showing relative abundance of the C_{27}, C_{28}, and C_{29} regular steranes in the saturated fraction of the Huhehu source rock extract

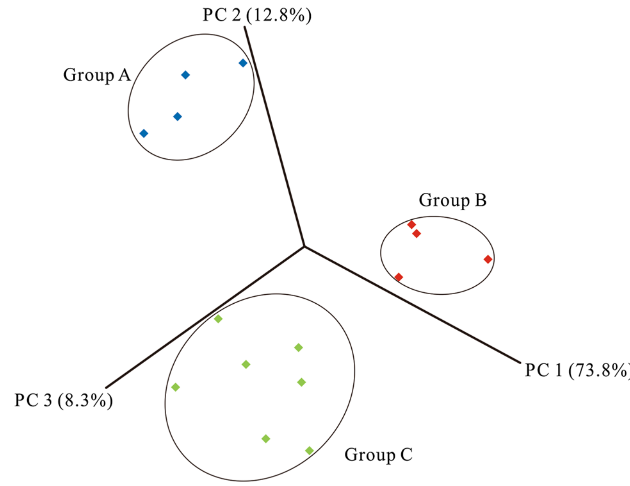

Fig. 9 Separation of the Huhehu oils into three different genetic oil families based on the principal component analysis (PCA) of nine source- and age-related biomarker ratios

the group C oils is linked to the K_1n_2 coal member (Fig. 15a). Figure 15b shows the relative contribution from each of the 11 biomarker ratios to PC1, PC2, and PC3. The biomarker ratios of Ts/(Ts + Tm) and C_{35}/C_{34} have large positive loadings on PC1. PC1 could be interpreted as an indicator of more reducing depositional conditions since the Ts/(Ts + Tm) ratio is a source-related parameter at lower maturity (Wang et al. 2018), and the C_{35}/C_{34} ratio generally reflects anoxic depositional conditions (Peters and Moldowan 1991). The loadings on PC2 are dominated by a positive correlation with C_{29} hopane/C_{30} hopane and C_{31} 22R/C_{30} hopane ratios and a negative correlation with $\%C_{27}$, which is indicative of more marine organic matter input (Huang and Meinschein 1979; Peters et al. 2005). The loadings on PC3 mainly show a positive correlation with Pr/Ph and $\%C_{29}$ and a negative correlation with $\%C_{27}$. Thus, PC3 indicates more oxic depositional conditions (Didyk et al. 1978) and terrigenous organic matter input (W Huang and Meinschein 1979).

Geological evidence also provides support for geochemical oil-source correlations in the Huhehu Sag. For example, the discovered oils are mainly distributed in wells He-2 and He-6 (Table 4). The burial depths of the coal seams in He-2 and He-6 are in the range of 570 to 1600 m and 570 to 1550 m (Qu 2005), respectively. Such evidence indicates that group A oils are mainly derived from the K_1n mudstone Formation rather than from the coal formation

Fig. 8 Separation of the Huhehu oils into three different genetic oil families based on the hierarchical cluster analysis of nine source- and age-related biomarker ratios

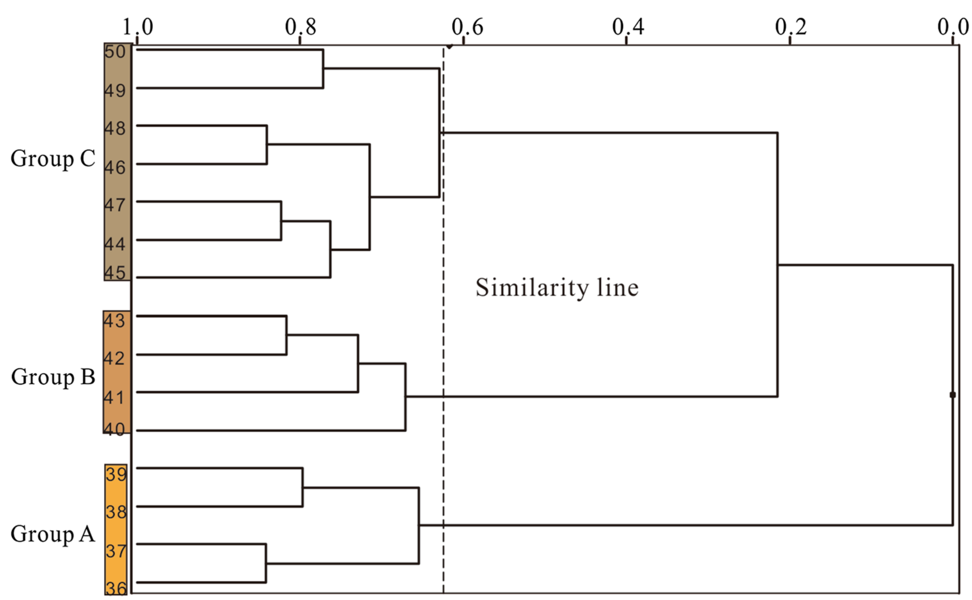

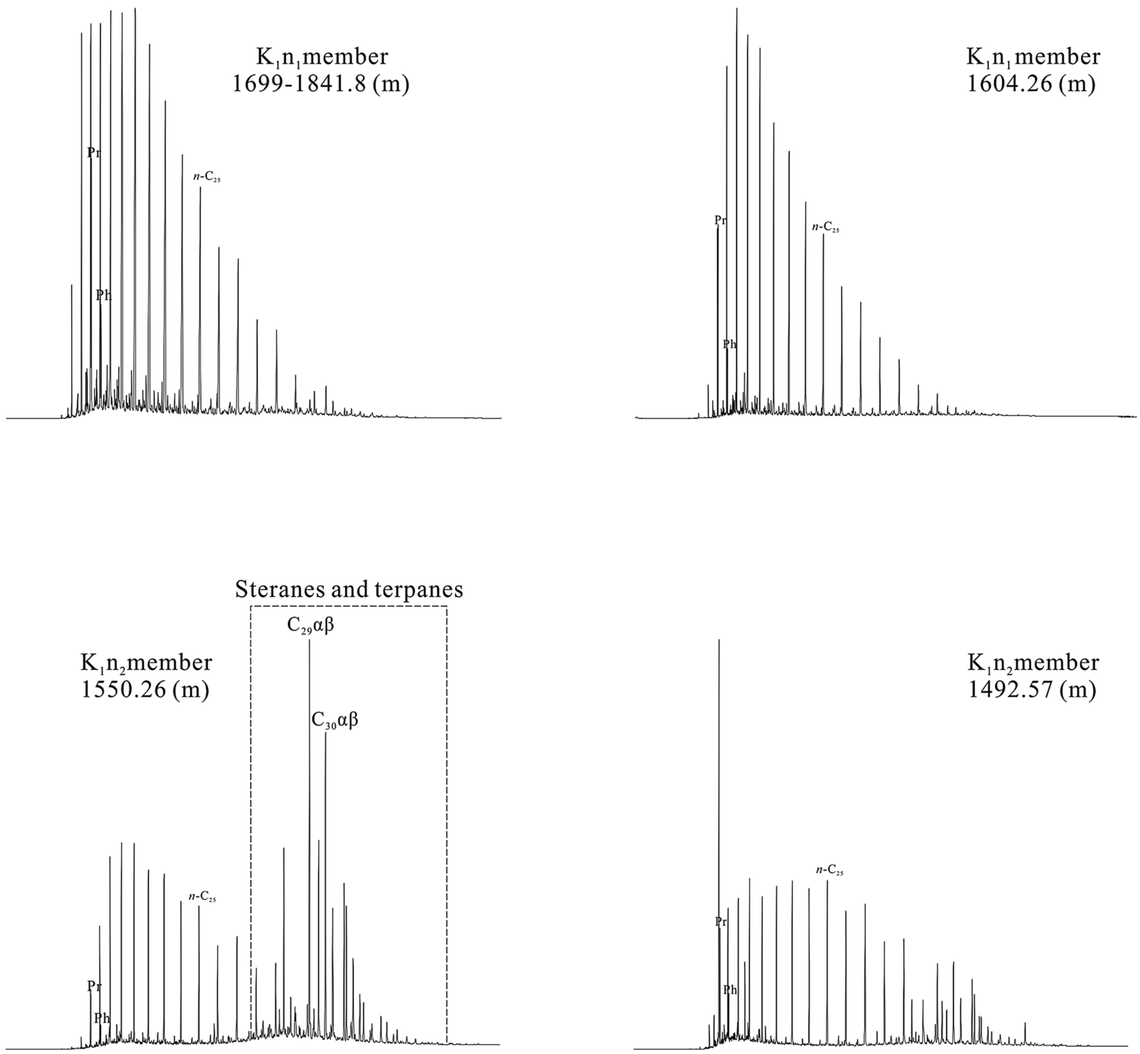

Fig. 10 Whole oil gas chromatograms of the Huhehu oils showing the relative distribution of *n*-paraffins

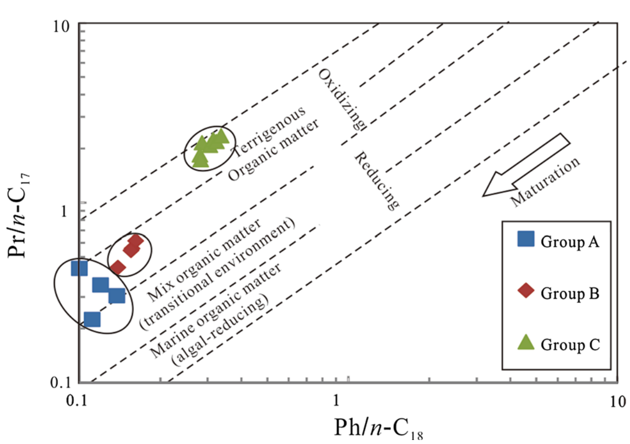

Fig. 11 Plot of Pr/*n*-C_{18} versus Ph/*n*-C_{17} for the Huhehu oils showing genetic oil categories and depositional conditions

because oils from group A have greater embedded depths (> 1600 m). In contrast, the depth of the group C oils is within the coal seam distribution. Accordingly, the group C oils have good correlation with the coal extracts from the K_1n_2 member.

The oil–source rock correlation results are consistent with the thermal maturity of the Huhehu oils and source rocks (Fig. 11). For example, the group A oils have relatively high maturity and show a strong affinity to the relatively high maturity source rocks of the K_1n_2 and K_1n_1 mudstone members. Similar observations could be made for the group B and group C oils.

As discussed earlier, the K_1d_1 and K_1n_2 mudstone samples have moderate to high hydrocarbon generative potential, while the K_1n_1 mudstone member and K_1n_2 and K_1n_1 coal samples are relatively less promising and show poor-to-good and poor-to-fair hydrocarbon generation potential, respectively. The K_1n_2 coal member has a certain hydrocarbon-generating potential, but the K_1n_1 coal member is less promising, which is consistent with a

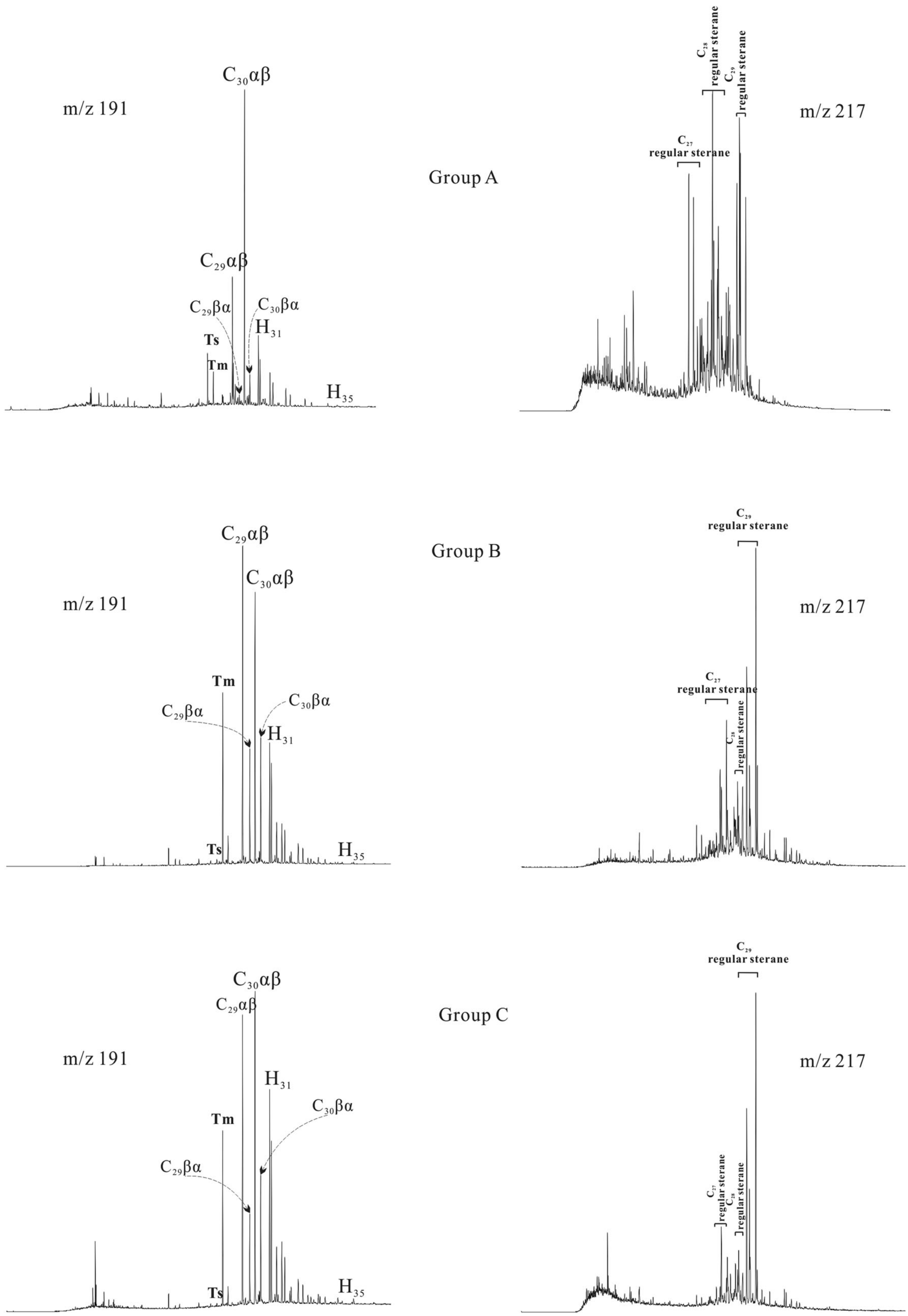

Fig. 12 Mass chromatograms (m/z 191 and 217) for the representative Huhehu oils

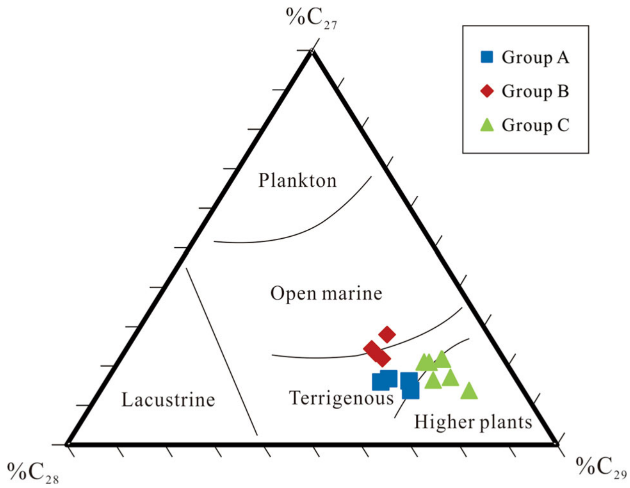

Fig. 13 Ternary diagram showing the relative abundance of the C_{27}, C_{28}, and C_{29} regular steranes in the saturated fraction of the Huhehu oils

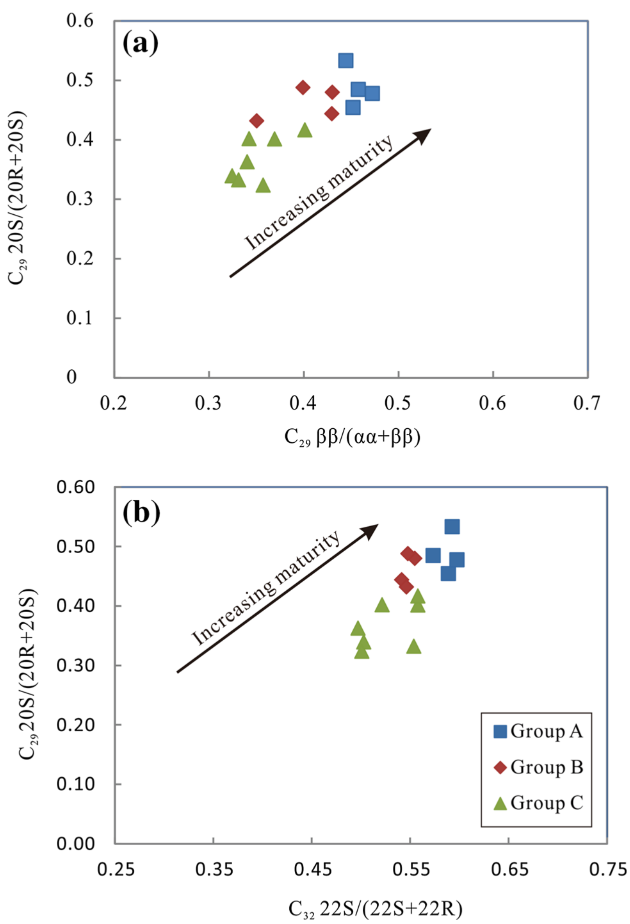

Fig. 14 Plots of C_{29} steranes ββ/(αα + ββ) versus C_{29} steranes 20S/(20R + 20S) (**a**) and C_{32} homohopane 22S/(22S + 22R) versus C_{29} steranes 20S/(20R + 20S) (**b**) showing thermal maturity level of the Huhehu oils

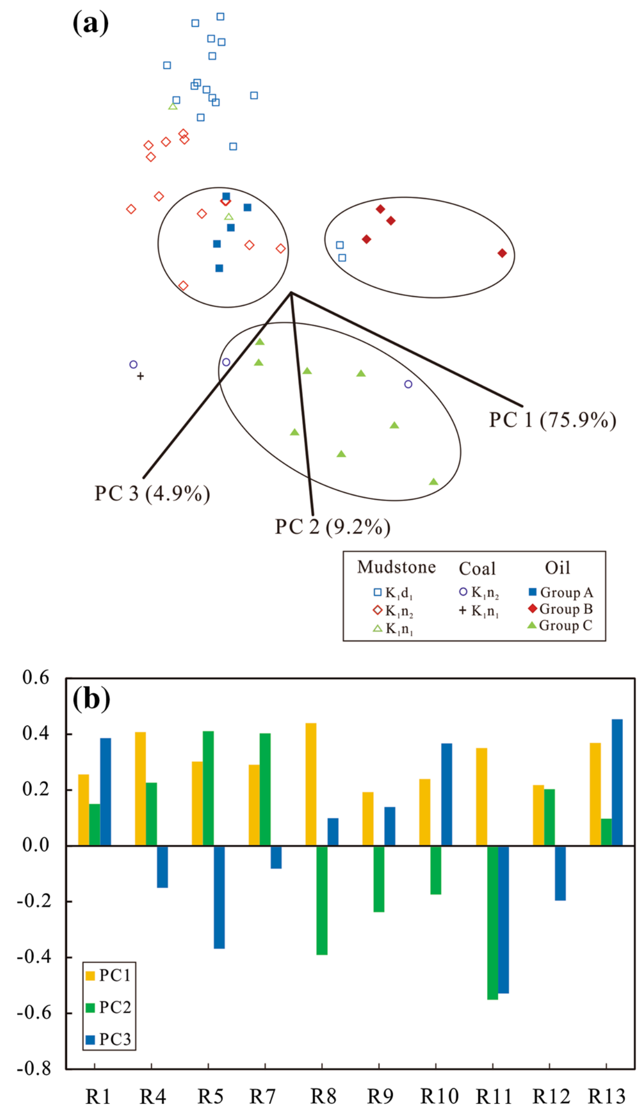

Fig. 15 The three Huhehu oil families (scores) and biomarker variables (loadings) employed in the principal component analysis. R1 = pristane/phytane; R4 = Ts/(Ts + Tm); R5 = C_{29} hopane/C_{30} hopane; R7 = C_{31} 22R/C_{30} hopane; R8 = C_{35}/C_{34} homohopanes; R9 = gammacerane/C_{31} 22R hopane; R10 = steranes/hopanes; R11 = %C_{27} (e.g., %C_{27} = %C_{27}/(%C_{27}–%C_{29}); R12 = %C_{28}; R13 = %C_{29}

previous study (Liu 2010). Therefore, the hydrocarbon generation potential of the source rocks supports the results of the oil–oil and oil–source rock correlations in the present study. Future assessment of petroleum potential or exploration of the Huhehu Sag can be assisted by considering the proposed genetic relationship between the crude oils and source rocks. The results of oil–oil and oil–source rock correlation in the Huhehu Sag suggest that the K_1n Formation and K_1d_1 member are promising for future exploration.

5 Conclusions

Based on Rock–Eval pyrolysis data, mudstones from the K_1d_1 and K_1n_2 members have moderate to high hydrocarbon generating potential, while the K_1n_1 mudstone member and coals from the K_1n_2 and K_1n_1 members in this region have relatively less potential.

Based on chemometric analysis and biomarker characteristics, we divided the Huhehu oils into three groups. Group A oils have relatively high maturity and are characterized by moderate values of Pr/Ph, low values of Pr/n-C_{17} and Ph/n-C_{18}, and moderate concentrations of C_{29} sterane, while group B oils have moderate maturity, low values of Pr/Ph, moderate values of Pr/n-C_{17} and Ph/n-C_{18}, and low concentrations of C_{29} sterane. Group C oils have low maturity; relatively high values of Pr/Ph, Pr/n-C_{17}, and Ph/n-C_{18}; and low concentrations of C_{29} sterane. The oil–source rock correlation based on PCA analysis suggests group A oils are derived from the K_1n_2 and K_1n_1 mudstone members, while group B oils can be ascribed to the K_1d_1 mudstone member, and group C oils to the K_1n_2 coal member. These results suggest that not only the K_1n Formation, but also the K_1d_1 member, are good prospects for hydrocarbon exploration.

Acknowledgements This study was funded by the Natural Science Funding Council of China (Grant Nos. 41273059), GIGCAS 135 project (Grant No. Y234021001) and Earmarked Fund of the State Key Laboratory of Organic Geochemistry (Grant No. sklog2016-A01). The authors are deeply indebted to two anonymous reviewers who provided constructive reviews in our original manuscript. We also wish to acknowledge managing editor Wang Binbin for the timely handling with the manuscript.

Compliance with ethical standards

Conflict of interest The authors declare that they have no conflict of interest.

References

Amiri V, Nakhaei M, Lak R (2017) Using radon-222 and radium-226 isotopes to deduce the functioning of a coastal aquifer adjacent to a hypersaline lake in NW Iran. J Asian Earth Sci 147:128–147

Brito M, Rodrigues R, Baptista R, Duarte LV, Azerêdo AC, Jones CM (2017) Geochemical characterization of oils and their correlation with Jurassic source rocks from the Lusitanian Basin (Portugal). Mar Pet Geol 85:151–176

Cao RC, Wang WM, Shang JH, Wang QK (2010) Research into hydrocarbon source rocks in Huhehu Depression by application of sequence stratigraphic geochemistry method. J Northeast Pet Univ 34:18–22 **(in Chinese with English abstract)**

Chakhmakhchev A, Suzuki N, Suzuki M, Takayama K (1996) Biomarker distributions in oils from the Akita and Niigata Basins, Japan. Chem Geol 133:1–14

Chen HP (2014) Geochemical characteristics and oil-source rock correlation of Nantun coal measure source rocks in Huhehu Sag. West-China Exploration Engineering, pp 50–57 (in Chinese)

Chen JP, Zhao CY, He ZH (1997) Criteria for evaluating the hydrocarbon-generating potential of organic matter in coal measures. Pet Explor Dev 24:1–5 **(in Chinese with English abstract)**

Chen JP, Zhao CY, Wang ZY, He ZH, Qin Y (1998) Organic geochemical characteristics of oil, gas and source rocks of Jurassic coal measures in Northwestern China. Geol Rev 44:149–159 **(in Chinese with English abstract)**

Chen JP, Wu HY, Zhu DF, Lin CH, Yu DS (2007) Tectonic evolution of the Hailar Basin and its potentials of oil-gas exploration. Chin J Geol 42:147–159 **(in Chinese with English abstract)**

Chen XH, Lu SF, Xue HT, Li JH, Liu QH, Hu SM, Huang WB (2011) Seismic facies of the Cretaceous in the Huhehu Depression, Hailar Basin. Pet Explor Dev 38:321–327 **(in Chinese with English abstract)**

Cui JP, Ren ZL, Su Y, Zhang S, Liu L (2007) Relationship between present geo-temperature and hydrocarbon generation in Hailar Basin. Pet Explor Dev 34:445–450 **(in Chinese with English abstract)**

Didyk BM, Simoneit BRT, Brassell SC, Eglinton G (1978) Organic geochemical indicators of palaeoenvironmental conditions of sedimentation. Nature 272:216–222

Ding H, Liu CQ, Zhao ZQ, Li SL, Lang YC, Li XD, Hu J, Liu BJ (2017) Geochemistry of the dissolved loads of the Liao River basin in northeast China under anthropogenic pressure: chemical weathering and controlling factors. J Asian Earth Sci 138:657–671

Dong L, Wang WM, Yu XB, Wang GH (2011) Study on hydrocarbon accumulation stages in Nantun Formation, Huhehu Depression, Hailar Basin. Pet Geol Recovery Effic 18:20–23 **(in Chinese with English abstract)**

Fu JM, Sheng GY, Peng PA, Brassell SC, Eglinton G, Jiang J (1986) Peculiarities of salt lake-sediments as potential source rocks in China. Org Geochem 10:119–126

Hao F, Zhou XH, Zhu YM, Bao XH, Yang YY (2009) Charging of the Neogene Penglai 19-3 field, Bohai Bay Basin, China: oil accumulation in a young trap in an active fault zone. Am Assoc Pet Geol Bull 93:155–179

Hao F, Zhou XH, Zhu YM, Zou HY, Yang YY (2010) Charging of oil fields surrounding the Shaleitian uplift from multiple source rock intervals and generative kitchens, Bohai Bay basin, China. Mar Pet Geol 27:1910–1926

Hao F, Zhang ZH, Zou HY, Zhang YC, Yang YY (2011) Origin and mechanism of the formation of the low-oil-saturation Moxizhuang field, Junggar Basin, China: implication for petroleum exploration in basins having complex histories. Am Assoc Pet Geol Bull 95:983–1008

He M, Moldowan JM, Nemchenko-Rovenskaya A, Peters KE (2012) Oil families and their inferred source rocks in the Barents Sea and northern Timan-Pechora Basin, Russia. Am Assoc Pet Geol Bull 96:1121–1146

Huang WY, Meinschein WG (1979) Sterols as ecological indicators. Geochim Cosmochim Acta 43:739–745

Huang DF, Xiong CW (1996) Generation, migration and evaluation of hydrocarbon generation potential of oil formed in coal-bearing strata. China Pet Exp 1:6–11 **(in Chinese with English abstract)**

Hunt JM (1996) Petroleum geochemistry and geology. W.H. Freeman, New York

Jiang ZL, Qiu HJ, Huang YP, Fu WK, Jiang KP, Chen J (2014) Jurassic lacustrine source rock characteristics and its petroleum geological significance in the Southeast Depression of Tarim Basin, China. Arab J Geosci 7:5093–5106

Li S, Mao XP, Tang DZ, Tao S, Yang WH (2009) Resource assessment of coal-derived in Huhehu Depression, Hailar Basin. Geol China 36:1350–1358 **(in Chinese with English abstract)**

Li JH, Lu SF, Meng QA, Liu QH, Chen XH, Hu SM (2010) Typical sand characteristic of Nantun Formation in the Huhehu Depression in the Hailar Basin. Acta Geol Sin 84:1495–1501 **(in Chinese with English abstract)**

Liu HY (2010) The evaluation of hydrocarbon source rock in Huhehu Depression. Dissertation, Daqing Petroleum Institute

Liu QH, Lu SF, Li JH, Chen XH, Hu SM (2010) Sequence stratigraphic and sedimentary system analysis of Nantun group in Huhehu Depression in Hailar Basin. Acta Geol Sin 28:227–234 **(in Chinese with English abstract)**

Lu K, Hou DJ, Hong HF, Cao HM (2010) Geochemical characteristics of crude oil and correlation of source rock in Huhehu Sag. J Guilin Univ Technol 30:28–32 **(in Chinese with English abstract)**

Mashhadi ZS, Rabbani AR, Kamali MR (2015) Geochemical characteristics and hydrocarbon generation modeling of the Kazhdumi (Early Cretaceous), Gurpi (Late Cretaceous) and Pabdeh (Paleogene) formations, Iranian sector of the Persian Gulf. Mar Pet Geol 66:978–997

Meng YL, Xu C, Xiao LH, Zhou XG, Hu AW (2014) Organic geochemistry of Lower Jurassic source rocks in Xining Basin. Nat Gas Geosci 25:588–594 **(in Chinese with English abstract)**

Peters KE (1986) Guidelines for evaluating petroleum source rock using programmed prolysis. Am Assoc Pet Geol Bull 70:318–329

Peters KE, Moldowan JM (1991) Effects of source, thermal maturity, and biodegradation on the distribution and isomerization of homohopanes in petroleum. Org Geochem 17:47–61

Peters KE, Walters CC, Moldowan JM (2005) The biomarker guide: biomarkers and isotopes in petroleum and earth history, 2nd edn. Cambridge University Press, Cambridge

Peters KE, Scott RL, Zumberge JE, Valin ZC, Scotese CR, Gautier DL (2007) Circum-Arctic petroleum systems identified using decision-tree chemometrics. Am Assoc Pet Geol Bull 91:877–913

Peters KE, Hostettler FD, Lorenson TD, Rosenbauer RJ (2008) Families of Miocene Monterey crude oil, seep, and tarball samples, coastal California. Am Assoc Pet Geol Bull 92:1131–1152

Peters KE, Coutrot D, Nouvelle X, Ramos LS, Rohrback BG, Magoon LB, Zumberge JE (2013) Chemometric differentiation of crude oil families in the San Joaquin Basin, California. Am Assoc Pet Geol Bull 97:103–143

Peters KE, Wright TL, Ramos LS, Zumberge JE, Magoon LB (2016) Chemometric recognition of genetically distinct oil families in the Los Angeles basin, California. Am Assoc Pet Geol Bull 100:115–135

Qu GN (2005) Study on the best object appreciation of coal-bed methane in the Huhehu Depression of Hailar Basin. Dissertation, Liaoning Technical University

Seifert WK, Moldowan JM (1978) Applications of steranes, terpanes and monoaromatics to the maturation, migration and source of crude oils. Geochim Cosmochim Acta 42:77–95

Seifert WK, Moldowan JM (1980) The effect of thermal stress on source-rock quality as measured by hopane stereochemistry. Phys Chem Earth 12:229–237

Seifert WK, Moldowan JM (1986) Use of biological markers in petroleum exploration. Methods Geochem Geophys 24:261–290

Sinninghe Damsté JS, Kenig F, Koopmans MP, Köster J, Schouten S, Hayes JM, de Leeuw JW (1995) Evidence for gammacerane as an indicator of water column stratification. Geochim Cosmochim Acta 59:1895–1900

Song HX, Wen ZG, Bao JP (2015) Geochemical characteristics and hydrocarbon potential of the coal in Muli area of Qilian Mountain. Nat Gas Geosci 26:1803–1813 **(in Chinese with English abstract)**

Telnæs N, Cooper BS (1991) Oil-source rock correlation using biological markers, Norwegian continental shelf. Mar Pet Geol 8:302–310

Tissot BP, Welte DH (1984) Petroleum formation and occurrence, 2nd edn. Springer, Berlin

Tissot BP, Pelet R, Ungerer P (1987) Thermal history of sedimentary basins, maturation indices and kinetics of oil and gas generation. Am Assoc Pet Geol Bull 71:1445–1466

Wang CJ (1998) A "folded-fan" method for assessment on the hydrocarbon-generating potential of coals. Geochimica 27:483–492 **(in Chinese with English abstract)**

Wang PJ, Zhong JH, Niu YB (2009) Tectonic feature and evolution of Huhehu Depression in Hailar Basin. Spec Oil Gas Reserv 16:25–27 **(in Chinese with English abstract)**

Wang YP, Zhang F, Zou YR, Zhan ZW, Peng PA (2016) Chemometrics reveals oil sources in the Fangzheng Fault Depression, NE China. Org Geochem 102:1–13

Wang YP, Zhang F, Zou YR, Lin XH, Liang T (2018) Oil source and charge in the Wuerxun Depression, Hailar Basin, northeast China: a chemometric study. Mar Pet Geol 89:665–686

Wu HB, Li JH (2012) Sequence stratigraphic geochemistry and its application to the evaluation of source rocks of Huhehu Sag in Hailar Basin. Acta Geol Sin 86:661–670 **(in Chinese with English abstract)**

Yang ZR, Zhang YF, Yao Y (2008) Potential analysis coalbed gas resources in Huhehu Depression, Hailar Basin. Coal Geol Explor 36:15–18 **(in Chinese with English abstract)**

Zhang F (2014) Geochemical characteristic and hydrocarbon-generating potential of coal-bearing source rock with middle to low rank, Huhehu Depression. Nat Gas Explor Dev 37:19–24 **(in Chinese with English abstract)**

Zhang MF, Xiong DL, Wu CJ, Ma WY, Sun LN, Tuo JC (2016) Source rock condition and the formation of Jurassic low-maturity gases in the eastern Junggar Basin. Nat Gas Geosci 27:261–267 **(in Chinese with English abstract)**

Zumberge JE, Russell JA, Reid SA (2005) Charging of Elk Hills reservoirs as determined by oil geochemistry. Am Assoc Pet Geol Bull 89:1347–1371